NASA
Contractor Report 195306

Army Research Laboratory
Contractor Report ARL–CR–145

Generation of Gear Tooth Surfaces by Application of CNC Machines

F.L. Litvin and N.X. Chen
University of Illinois at Chicago
Chicago, Illinois

April 1994

429271

Prepared for
Lewis Research Center
Under Grant NAG3–1263

National Aeronautics and
Space Administration

U.S. ARMY
RESEARCH LABORATORY

Generation of Gear Tooth Surfaces by Application of CNC Machines

F.L. Litvin and N.X. Chen
The University of Illinois at Chicago
Chicago, Illinois 60680

Summary

This study will demonstrate the importance of application of CNC machines in generation of gear tooth surfaces with new topology. This topology decreases gear vibration and will extend the gear capacity and service life. A preliminary investigation by a tooth contact analysis(TCA) program has shown that gear tooth surfaces in line contact (for instance, involute helical gears with parallel axes, worm-gear drives with cylindrical worms etc.) are very sensitive to angular errors of misalignment that cause edge contact and an unfavorable shape of transmission errors and vibration.

The new topology of gear tooth surfaces is based on the localization of bearing contact, and the synthesis of a predesigned parabolic function of transmission errors that is able to absorb a piecewise linear function of transmission errors caused by gear misalignment.

The report will describe the following topics: (1) Description of kinematics of CNC machines with 6 degrees-of-freedom that can be applied for generation of gear tooth surfaces with new topology. (2) A new method for grinding of gear tooth surfaces by a cone surface or surface of revolution based on application of CNC machines. This method provides an

optimal approximation of the ground surface to the given one. This method is especially beneficial when undeveloped ruled surfaces are to be ground. (3) Execution of motions of the CNC machine. The solution to this problem can be applied as well for the transfer of machine-tool settings from a conventional generator to the CNC machine.

The developed theory required the derivation of a modified equation of meshing based on application of the concept of space curves, space curves represented on surfaces, geodesic curvature, surface torsion etc. Condensed information on these topics of differential geometry is provided as well.

Introduction

The design and manufacture of gears with new topology of gear tooth surfaces are problems of great importance for helicopter transmissions. The existing technology of gears is restricted with the necessity to use cutting and grinding machines whose kinematics is based on linear relations between the motions of the tool and the workpiece.

The need of low-noise gears with increased load capacity and service life can be satisfied with a new topology of gear tooth surfaces that is able to provide: (i) a reduced sensitivity to misalignment and avoidance of edge contact, (ii) a parabolic type of function of transmission errors to reduce the level of possible vibration, (iii) a localized bearing contact with controlled dimensions of the instantaneous contact ellipse.

The application of CNC (Computer Numerically Controlled) machines overcomes the obstacles presented for generation of gears with a new surface topology by using the existing equipment. The CNC machines are able to provide computer controlled nonlinear relations between the motions of the tool and the gear being generated. Although such machines are used at present mainly for the installment of machine-tool settings with higher precision, their prosperous future is in their application for generation of gears with new topology. The

CNC machines are a unique opportunity for researchers to modify the geometry of traditional gear drives and benefit industry with gear drives with substantially improved parameters.

The modification of geometry of gear tooth surfaces requires from researchers a new approach for the development of principles of conjugation of gear tooth surfaces. Application of conjugate gear tooth surfaces being in instantaneous line contact is in the authors' opinion an anachronism. Such gear tooth surfaces are very sensitive to misalignment that causes the shift of the bearing contact to the edge and transmission errors of such a type that cause a jerk at the transfer from one cycle of meshing to the next. The considerations above are true for spur gears, involute helical gears with parallel axes, and worm-gear drives.

It is necessary as well to change the attitude to some finishing processes such as honing and shaving applied for helical and spur gears. It is not reasonable to require that such finishing processes would provide the exact screw involute surfaces knowing ahead that only modified tooth surfaces are to be applied.

The statements mentioned above are illustrated with the following drawings.

Figures 1 to 4 show the influence of angular errors of misalignment $\Delta\gamma$ and $d\lambda_{pi}$ of involute helical gears with parallel axes that cause edge contact (figures 1 and 3) and piecewise almost linear functions of transmission errors (figures 2 and 4). The drawings above are based on the investigation performed by Reference [1]. The design parameters of the helical gears are shown below:

$$
\begin{aligned}
N_1 &= 20 \\
N_2 &= 40 \\
P_n &= 1.1985\ (\frac{1}{mm}) \\
\alpha_n &= 20^\circ \\
\beta_p &= 30^\circ \\
\text{Tooth face width, } F_N, &= 40.64(mm)
\end{aligned}
$$

Figures 5, 6 and 7 illustrate the impact of misalignment of worm-gear drives. The shift

of the bearing contact is shown in figures 5 and 6, and the undesirable shift of transmission errors is shown in figure 7 that will inevitable cause vibration. The drawings are based on the research accomplished by Reference [2].

The design parameters of the worm-gear drive are shown below:

N_1	=	2
N_2	=	30
Axial module, m	=	$8(mm)$
γ	=	90°
Shortest distance, E,	=	$176(mm)$

Figure 8 illustrates why a predesigned parabolic type of transmission errors is beneficial for the gears with the new topology (Ref. [3]). This figure illustrates the interaction of a parabolic function of transmission errors(provided at the stage of synthesis of the gear tooth surfaces) with a linear function of transmission errors(caused by misalignment). The combination of these functions is again a parabolic function, with the same slope as the predesigned one that is translated with respect to the initial parabolic function. This means that the predesigned parabolic function absorbs the linear function and keeps the shape of a parabolic function.

There are three cases of generation of the workpiece surface Σ_p by the given tool surface Σ_t by CNC machines:

(1) Surfaces Σ_t and Σ_p are in continuous tangency, however they contact each other at every instant at a *point* not a line.

(2) Surfaces Σ_t and Σ_p are in continuous tangency and they contact each other at every instant at a *line*. Surface Σ_p is generated in this case as the *envelope* to the *family* of surfaces Σ_t. The family of surfaces is generated in *relative* motion of Σ_t to Σ_p.

(3) An approximate method for generation of a surface Σ_g (ground or cut) with an optimal

approximation to the ideal surface Σ_p.

An example of case 1 is the generation, for instance, of a die designed for forging of a gear. Generation of conventional spiral bevel gears and hypoid gears by the "Phoenix" machine is the example of case 2 generation. Case 3 is the basic idea for a new method for surface generation discussed in section 4. Only cases 2 and 3 of surface generation are discussed in this report.

The contents of the report covers the following topics:

(i) Description of "Phoenix" and "Star" CNC machines, that are suitable for generation of gear tooth surfaces with new topology.

(ii) Execution of motions of CNC machines.

(iii) Generation of a surface with optimal approximation to the ideal surface.

(iv) Concept of curvatures that are required for computations for the proposed approach for generation.

1. "Phoenix" and "Star" CNC Machines

"Phoenix" CNC Machine

The "Phoenix" CNC machine (figure 9) is designed by the Gleason Works for generation of spiral bevel and hypoid gears. The machine is provided with a total of six degrees-of-freedom. Three rotational motions, and three translational motions are used. The translational motions are performed in three mutually perpendicular directions. Two of rotational motions are provided as rotation of the workpiece and the rotation that enables to change the angle between the axes of the workpiece and the tool. The sixth rotational motion is

provided as rotation of the tool about its axis, and generally is not related with the process for generation. The motions with other five degrees-of-freedom are provided as related motions in the process for surface generation.

Coordinate Systems Applied for "Phoenix"

Coordinate systems S_t (x_t, y_t, z_t) and S_p (x_p, y_p, z_p) are rigidly connected to the tool and the workpiece, respectively (figure 10). For further discussions we will distinguish four reference frames designated in figure 9 as I, II, III and IV. The reference frame IV is the fixed one to the housing of the machine. Reference frames I, II and III perform translations in three mutually perpendicular directions, respectively. We designate coordinate systems S_h and S_m that represent reference frames I and III, respectively(figures 9 and 10). Coordinate axes of S_h and S_m are parallel to each other and the location of S_h with respect to S_m is represented by ($x_m^{(O_h)}$, $y_m^{(O_h)}$, and $z_m^{(O_h)}$). Coordinate system S_t performs rotational motion with respect to S_h about the z_h-axis. To describe the coordinate transformation from S_m to S_p, we use coordinate systems S_e and S_d(figure 10). Coordinate system S_e performs rotation with respect to S_m about the y_m-axis. Coordinate axes of system S_d are parallel to the respective axes of S_e; the location of origin O_d with respect to O_e is determined with the parameter $x_d^{(O_d)}$ = const. Coordinate system S_p performs rotational motion with respect to S_d about the x_d-axis.

"Star" CNC Machine

A version of the "Star" CNC machine that is provided with 6 degrees-of-freedom is shown in figure 11. Coordinate systems S_t (x_t, y_t, z_t), S_p (x_p, y_p, z_p) and S_f (x_f, y_f, z_f) are rigidly connected to the tool, workpiece and frame, respectively. Coordinate system S_d is parallel to system S_f and the location of S_d with respect to S_f is represented in S_f by ($x_f^{(O_d)}$, 0, 0). Coordinate system S_e performs rotational motion with respect to S_d about the y_d-axis. Coordinate system S_h is parallel to S_e and the location of S_h with respect to S_e is represented

in S_e by $(0, y_e^{(O_h)}, z_e^{(O_h)})$. Coordinate system S_t performs rotational motion with respect to S_h about the x_h-axis. Coordinate system S_p performs rotational motion with respect to the fixed coordinate system S_f about the x_f-axis. Altogether there are three translational motions along axes x_f, y_e and z_e and three rotational motions about axes x_f, y_d, and x_h.

2. Basic Principle of Execution of Motions on CNC Machine

Consider that the location and orientation of the tool with respect to the workpiece are given in coordinate systems that are represented for a conventional generator or for an abstract(mathematical) model of the process for generation. We will consider for the following derivations the example of application of the "Phoenix" machine. A similar approach can be applied for other types of CNC machines, for instance, for the "Star" machine. Our goal is to develop the algorithm for the execution of motions of the CNC machine using the initial information mentioned above. Reference [4] has used for this purpose the existence of a common trihedron for the two couples of coordinate systems $(S_t^{(C)}, S_p^{(C)})$ and $(S_t^{(G)}, S_p^{(G)})$ that are applied for the CNC machine and for the generating process, respectively. The approach used in this report is as follows:

(i) Consider that 4×4 matrices $\mathbf{M}_{pt}^{(k)}$ and 3×3 matrices $\mathbf{L}_{pt}^{(k)}$ $(k = C,\ G)$ have been derived. The superscripts "C" and "G" indicate the CNC machine and the abstract generating process, respectively.

(ii) The matrix equality

$$\mathbf{L}_{pt}^{(C)} = \mathbf{L}_{pt}^{(G)} \tag{1}$$

will provide the same orientation of $S_t^{(k)}$ with respect to $S_p^{(k)}$ $(k = C,\ G)$ in both reference frames.

(iii) The matrix equality

$$\mathbf{M}_{pt}^{(C)}[\ 0\ \ 0\ \ 0\ \ 1\ ]^T = \mathbf{M}_{pt}^{(G)}[\ 0\ \ 0\ \ 0\ \ 1\ ]^T \tag{2}$$

will provide the same position vector $(\overline{O_pO_t})_p$ for both reference frames.

The application of equations (1) and (2) for the execution of motions of the "Phoenix" machine is considered for the two following cases: (i) a hypoid pinion is generated by application of a conventional generator, and (ii) a surface Σ_g with optimal approximation to the ideal surface Σ_p is generated.

Derivation of Matrix $\mathbf{L}_{pt}^{(C)}$ and Position Vector $(\overline{O_tO_p})_p^{(C)}$

Using a routine procedure for coordinate transformations, we obtain

- $$\mathbf{L}_{pt}^{(C)}(\mu,\phi,\psi) = \mathbf{L}_{pd}(\psi)\mathbf{L}_{de}\mathbf{L}_{em}(\phi)\mathbf{L}_{mh}\mathbf{L}_{ht}(\mu)$$

$$= \begin{bmatrix} \cos\mu\cos\phi & -\sin\mu\cos\phi & \sin\phi \\ -\cos\mu\sin\phi\sin\psi + \sin\mu\cos\psi & \sin\mu\sin\phi\sin\psi + \cos\mu\cos\psi & \cos\phi\sin\psi \\ -\cos\mu\sin\phi\cos\psi - \sin\mu\sin\psi & \sin\mu\sin\phi\cos\psi - \cos\mu\sin\psi & \cos\phi\cos\psi \end{bmatrix} \tag{3}$$

We note that $\mathbf{L}_{de}$ and $\mathbf{L}_{mh}$ are unit matrices.

The derivation of the position vector $(\overline{O_tO_p})_p^{(C)}$ in S_p is based on the following considerations:

(i)

$$(\overline{O_m O_t})_p^{(C)} + (\overline{O_t O_p})_p^{(C)} = (\overline{O_m O_p})_p^{(C)}$$

Thus:

$$(\overline{O_t O_p})_p^{(C)} = (\overline{O_m O_p})_p^{(C)} - (\overline{O_m O_t})_p^{(C)} = (\overline{O_e O_d})_p^{(C)} - (\overline{O_m O_h})_p^{(C)}$$

$$= x_e^{(O_d)}(\mathbf{i}_e)_p - x_m^{(O_h)}(\mathbf{i}_m)_p - y_m^{(O_h)}(\mathbf{j}_m)_p - z_m^{(O_h)}(\mathbf{k}_m)_p \tag{4}$$

Here: $x_d^{(O_d)} = \text{const.}$, $x_m^{(O_h)}$, $y_m^{(O_h)}$ and $z_m^{(O_h)}$ are considered as algebraic values.

(ii) Vector $(\overline{O_t O_p})^{(C)}$ can be represented in coordinate system $S_p^{(C)}$ with the following matrix equation

$$(\overline{O_t O_p})_p^{(C)} = x_e^{(O_d)}\mathbf{i}_p - x_m^{(O_h)}\mathbf{L}_{pm}[\,1\;\;0\;\;0\,]^T$$

$$- y_m^{(O_h)}\mathbf{L}_{pm}[\,0\;\;1\;\;0\,]^T - z_m^{(O_h)}\mathbf{L}_{pm}[\,0\;\;0\;\;1\,]^T \tag{5}$$

where $\mathbf{L}_{pm} = \mathbf{L}_{pd}\mathbf{L}_{de}\mathbf{L}_{em}$ ($\mathbf{L}_{de}$ is a unitary matrix).

Equation (5) yields

$$(\overline{O_t O_p})_p^{(C)} = \begin{bmatrix} x_e^{(O_d)} - x_m^{(O_h)}\cos\phi - z_m^{(O_h)}\sin\phi \\ x_m^{(O_h)}\sin\phi\sin\psi - y_m^{(O_h)}\cos\psi - z_m^{(O_h)}\cos\phi\sin\psi \\ x_m^{(O_h)}\sin\phi\cos\psi + y_m^{(O_h)}\sin\psi - z_m^{(O_h)}\cos\phi\cos\psi \end{bmatrix} \tag{6}$$

3. Example: Generation of Hypoid Pinion by "Phoenix"

Generation of Pinion Tooth Surface by Conventional Generator

The pinion tooth surface is generated as the envelope to the family of tool surfaces that are cone surfaces as shown in figure 12.

Henceforth, we will consider the following coordinate systems: (i) the fixed ones, S_o and S_q that are rigidly connected to the cutting machine (figures 13 and 14); (ii) the movable coordinate systems S_c and S_p that are rigidly connected to the cradle of cutting machine and the pinion, respectively; (iii) coordinate system S_t that is rigidly connected to the head cutter. In the process of generation the cradle with S_c performs rotational motion about the z_o-axis with angular velocity $\omega^{(c)}$, and the pinion with S_p performs rotational motion about the x_q-axis with angular velocity $\omega^{(p)}$ (figure 14).

The tool (head-cutter) is mounted on the cradle and performs rotational motion *with* the cradle. Coordinate system S_t is rigidly connected to the cradle. To describe the installment of the tool with respect to the cradle we use coordinate system S_b (figures 12 and 13). The required orientation of the head-cutter with respect to the cradle is accomplished as follows: (i) coordinate systems S_b and S_t are rigidly connected and then they are turned as one rigid body about the z_c-axis through the swivel angle $j = 2\pi - \delta$ (figure 13); (ii) then the head-cutter with coordinate system S_t is tilted about the y_b-axis under the angle i (figure 12(b)). The head-cutter is rotated about its axis z_t but the angular velocity in this motion is not related with the generation process and depends only on the desired velocity of cutting.

The pinion setting parameters are E_m– the machine offset, γ_m– the machine-root angle, ΔB– the sliding base, and ΔA– the machine center to back are shown in figure 14. The head-cutter settings parameters are S_R– radial setting, θ_c– initial value of cradle angle, j– the swivel angle(figure 13), and i– the tilt angle(figure 12(b)).

Pinion Tool Surface Equations

The head-cutter surface is a cone and is represented in S_t (figure 12(a)) as

$$\mathbf{r}_t(s,\theta) = \begin{bmatrix} (r_c + s\sin\alpha)\cos\theta \\ (r_c + s\sin\alpha)\sin\theta \\ -s\cos\alpha \\ 1 \end{bmatrix} \tag{7}$$

Here: (s,θ) are the Gaussian coordinates, α is the blade angle and r_c is the cutter point radius. Vector function (7) with α positive and α negative represents surfaces of two head-cutters that are used to cut the pinion concave side and convex side, respectively.

The unit normal to the head-cutter surface is represented in S_t by the equations

$$\mathbf{n}_t = [\ -\cos\alpha\cos\theta \quad -\cos\alpha\sin\theta \quad -\sin\alpha\ ]^T \tag{8}$$

The family of tool surfaces is represented in S_p by the matrix equation

$$\mathbf{r}_p(s,\theta,\phi_p) = \mathbf{M}_{pq}\ \mathbf{M}_{qn}\ \mathbf{M}_{no}\ \mathbf{M}_{oc}\ \mathbf{M}_{cb}\ \mathbf{M}_{bt}\ \mathbf{r}_t(s,\theta) \tag{9}$$

Here: S_n is an auxiliary fixed coordinate system whose axes parallel to S_o axes.

$$\mathbf{M}_{bt} = \begin{bmatrix} \cos i & 0 & \sin i & 0 \\ 0 & 1 & 0 & 0 \\ -\sin i & 0 & \cos i & 0 \\ 0 & 0 & 0 & 1 \end{bmatrix}$$

$$\mathbf{M}_{cb} = \begin{bmatrix} -\sin j & -\cos j & 0 & S_R \\ \cos j & -\sin j & 0 & 0 \\ 0 & 0 & 1 & 0 \\ 0 & 0 & 0 & 1 \end{bmatrix}$$

$$\mathbf{M}_{oc} = \begin{bmatrix} \cos q & \sin q & 0 & 0 \\ -\sin q & \cos q & 0 & 0 \\ 0 & 0 & 1 & 0 \\ 0 & 0 & 0 & 1 \end{bmatrix}$$

$$\mathbf{M}_{no} = \begin{bmatrix} 1 & 0 & 0 & 0 \\ 0 & 1 & 0 & E_m \\ 0 & 0 & 1 & -\triangle B \\ 0 & 0 & 0 & 1 \end{bmatrix}$$

$$\mathbf{M}_{qn} = \begin{bmatrix} \cos\gamma_m & 0 & \sin\gamma_m & -\triangle A \\ 0 & 1 & 0 & 0 \\ -\sin\gamma_m & 0 & \cos\gamma_m & 0 \\ 0 & 0 & 0 & 1 \end{bmatrix}$$

$$\mathbf{M}_{pq} = \begin{bmatrix} 1 & 0 & 0 & 0 \\ 0 & \cos\phi_p & -\sin\phi_p & 0 \\ 0 & \sin\phi_p & \cos\phi_p & 0 \\ 0 & 0 & 0 & 1 \end{bmatrix}$$

$\delta = 2\pi - j$; $q = \theta_c + m_{cp}\phi_p$ where θ_c is the initial cradle angle and $m_{cp} = \omega^{(c)}/\omega^{(p)}$.

Equation of Meshing

This equation is described in Reference [5] as:

$$\mathbf{n}^{(p)} \cdot \mathbf{v}^{(cp)} = \mathbf{N}^{(p)} \cdot \mathbf{v}^{(cp)} = f(s, \theta, \phi_p) = 0 \tag{10}$$

where $\mathbf{n}^p$ and $\mathbf{N}^p$ are the unit normal and the normal to the tool surface, and $\mathbf{v}^{(cp)}$ is the relative velocity between the tool surface and the workpiece.

Equation (10) is invariant with respect to the coordinate system where the vectors of the scalar product are represented. These vectors in our derivations have been represented in S_o as follows,

$$\mathbf{n}_o = \mathbf{L}_{oc}\ \mathbf{L}_{cb}\ \mathbf{L}_{bt}\ \mathbf{n}_t$$

$$\mathbf{v}_o^{(cp)} = [(\ \boldsymbol{\omega}_o^{(c)} - \ \boldsymbol{\omega}_o^{(p)}) \times \mathbf{r}_o] + (\overline{O_oA} \times\ \boldsymbol{\omega}_o^{(p)})$$

Here:

$$\mathbf{r}_o = \mathbf{M}_{oc}\ \mathbf{M}_{cb}\ \mathbf{M}_{bt}\ \mathbf{r}_t$$

$$\overline{O_oA} = [\ 0 \quad -E_m \quad \Delta B\ ]^T$$

$$\boldsymbol{\omega}_o^{(p)} = -[\ \cos\gamma \quad 0 \quad \sin\gamma\ ]^T \quad ; \quad (|\ \boldsymbol{\omega}_o^{(p)}| = 1)$$

$$\boldsymbol{\omega}_o^{(c)} = -[\ 0 \quad 0 \quad m_{cp}\ ]^T$$

Pinion Tooth Surface

Equations (9) and (10) represent the pinion tooth surface in three-parametric form with parameters s, θ and ϕ_p. However, since equation (10) is linear with respect to s we can eliminate s and represent the pinion tooth surface in two-parametric form as

$$\mathbf{r}_p(\theta, \phi_p, d_k) \tag{11}$$

Here: d_k $(k = 1, \ldots, 8)$ designate the installment parameters: E_m, γ_m, ΔB, ΔA, S_R, θ_c, j and i.

The normal to the pinion tooth surface is represented as

$$\mathbf{n}_p(\theta, \phi_p, d_k) \tag{12}$$

where d_k $(k = 1, 2, 3, 4)$ designate the installment parameters γ_m, θ_c, j and i.

Derivation of $\mathbf{L}_{pt}^{(G)}$ and $(\overline{O_t O_p})_p^{(G)}$

Our next goal is to derive the algorithm for execution of motions on "Phoenix ", knowing the basic machine-tool settings on the conventional generator.

The coordinate systems applied for the CNC machine are represented in figure 10. The performed coordinate transformation yields:

$$(\mathbf{L}_{pt})^{(G)} = [a_{kl}(q)] \qquad (k = 1, 2, 3; l = 1, 2, 3) \tag{13}$$

Here:

$$\left.\begin{aligned}
a_{11} &= \cos i \cos\gamma_m \sin(q - j) - \sin i \sin\gamma_m \ , \\
a_{12} &= -\cos(q - j) \cos\gamma_m \ , \\
a_{13} &= \sin i \cos\gamma_m \sin(q - j) + \cos i \sin\gamma_m \ , \\
a_{21} &= \cos i \sin\gamma_m \sin\phi_p \sin(q - j) + \cos i \cos(q - j) \cos\phi_p \\
&\quad + \sin i \cos\gamma_m \sin\phi_p \ , \\
a_{22} &= -\cos(q - j) \sin\gamma_m \sin\phi_p + \sin(q - j) \cos\phi_p \ , \\
a_{23} &= \sin i \sin\gamma_m \sin\phi_p \sin(q - j) + \sin i \cos(q - j) \cos\phi_p \\
&\quad - \cos i \cos\gamma_m \sin\phi_p \ , \\
a_{31} &= -\cos i \sin\gamma_m \cos\phi_p \sin(q - j) + \cos i \cos(q - j) \sin\phi_p \\
&\quad - \sin i \cos\gamma_m \cos\phi_p \ , \\
a_{32} &= \sin\gamma_m \cos\phi_p \cos(q - j) + \sin(q - j) \sin\phi_p \ , \\
a_{33} &= -\sin i \sin\gamma_m \sin(q - j) \cos\phi_p + \sin i \cos(q - j) \sin\phi_p \\
&\quad + \cos i \cos\gamma_m \cos\phi_p
\end{aligned}\right\} \tag{14}$$

The variable parameters q and ϕ_p are related and therefore the coefficients a_{kl} ($k = 1,2,3; l = 1,2,3$) are functions of q.

The position vector $(\overline{O_tO_p})_p^{(G)}$ is represented as follows:

$$(\overline{O_tO_p})_p^{(G)} = -(\mathbf{M}_{pt})^{(G)}[\ 0\ \ 0\ \ 0\ \ 1\ ]^T$$

$$= -\begin{bmatrix} S_R\cos q\cos\gamma_m - \Delta B\sin\gamma_m - \Delta A \\ -S_R(\sin q\cos\phi_p - \cos q\sin\gamma_m\sin\phi_p) \\ \quad +E_m\cos\phi_p + \Delta B\cos\gamma_m\sin\phi_p \\ -S_R(\sin q\sin\phi_p + \cos q\sin\gamma_m\cos\phi_p) \\ \quad +E_m\sin\phi_p - \Delta B\cos\gamma_m\cos\phi_p \\ 1 \end{bmatrix}$$

$$= -\begin{bmatrix} a_{14}(q) \\ a_{24}(q) \\ a_{34}(q) \\ 1 \end{bmatrix} \tag{15}$$

Execution of Motions of CNC

Matrix equality (equation (1)) provides nine dependent equations for determination of functions $\phi(q)$, $\psi(q)$, and $\mu(q)$. We can determine these functions using the following procedure:

Step 1: Determination of ϕ.

$$\sin\phi = a_{13}(q) \tag{16}$$

This equation provides two solutions ϕ; the smaller value of ϕ can be chosen.

Step 2: Determination of ψ.

$$\cos\phi\sin\psi = a_{23}(q)\ , \qquad \cos\phi\cos\psi = a_{33}(q) \tag{17}$$

These equations provide a unique solution for ψ, considering ϕ as given.

Step 3: Determination of μ.

$$\cos\mu\cos\phi = a_{11}(q)\ , \qquad -\sin\mu\cos\phi = a_{12}(q) \tag{18}$$

These equations provide a unique solution for μ, considering ϕ as given.

For the generation a face-milled hypoid pinion, a tool with a cone surface is applied. The tool surface is a surface of revolution and the rotation of the tool about its axis is not related with ϕ. Functions (17) must be applied and executed only for the generation of face-hobbed hypoid pinion, that is cut by a blade.

Vector equality

$$(\overline{O_tO_p})_p^{(G)} = (O_tO_p)_p^{(C)} \tag{19}$$

permits the determination of functions $x_m^{(O_h)}(q)$, $y_m^{(O_h)}(q)$, and $z_m^{(O_h)}(q)$. Equations (6), (15) and (19) considered simultaneously, represent a system of three linear equations in the unknowns: $x_m^{(O_h)}$, $y_m^{(O_h)}$, $z_m^{(O_h)}$. The solution to these equations enables to determine the translational motions on the CNC machine.

4. Generation of a Surface with Optimal Approximation To the Ideal Surface

Introduction

This section is based on the research accomplished by Reference [2] that was directed at generation of a surface (Σ_g) that must be in optimal approximation to the theoretical (ideal) surface Σ_p.

The method for generation of Σ_g is based on following ideas:

(1) A mean line L_m on the ideal surface Σ_p is chosen as shown in figure 15.

(2) The tool surface Σ_t is a properly designed surface of revolution (in particular cases Σ_t is a circular cone as shown in figure 15) that moves along L_m. Surfaces Σ_t and Σ_p are in continuous tangency along L_m; M is the current point of tangency (figure 15). The orientation of Σ_t with respect to Σ_p (determined with angle β) is continuously varying. Angle β at current point M of tangency is formed by the tangents $\mathbf{t}_f$ and $\mathbf{t}_b$ to L_m and the tool generatrix, respectively (figure 15). Tangents $\mathbf{t}_f$ and $\mathbf{t}_b$ form plane Π that is tangent to Σ_t and Σ_p at point M.

(3) The tool surface Σ_t in its motion with respect to Σ_p swept out a region of space as a family of surfaces Σ_t. The envelope to the family of Σ_t is surface Σ_g, the ground or cut surface, that is in tangency with the theoretical surface Σ_p at any point M of L_m and must be in optimal approximation to Σ_p in any direction that differs from L_m.

(4) The optimal approximation of Σ_g to Σ_p is obtained by variation of angle β (figure 15).

(5) The continuous tangency of tool surface Σ_t with Σ_p and properly varied orientation of Σ_t can be obtained by the execution of required motions of the tool by a computer controlled multi-degree-of-freedom machine. One of these degrees of freedom, rotation of the tool about its axis, provides the desired velocity of grinding (cutting) and is not related with the process for generation of Σ_g.

The contents of this section cover the following topics:

(1) Determination of equation of meshing between the tool surface Σ_t and the generated surface Σ_g. The equation of meshing provides the necessary condition of envelope existence to the family of surfaces.

(2) Determination of generated surface Σ_g as the envelope to the family of surfaces Σ_t swept out by the tool. Surface Σ_g coincides with the theoretical (ideal) surface Σ_p along the mean line L_m and deviates from Σ_p out of L_m.

(3) Determination of deviations of Σ_g from Σ_p (in regions that differ from L_m) and minimizations of Σ_g deviations for optimal approximation of Σ_g to Σ_p.

(4) Determination of curvatures of Σ_g that are required when the simulation of meshing and contact of two mating surfaces are considered.

(5) Execution of required motions of Σ_t with respect to Σ_p by application of a multi-degree-freedom, computer numerically controlled machine.

An effective approach for the derivation of the necessary condition of the envelope Σ_g existence is discussed. This method is based on the idea of motion of the Darboux-Frenet trihedron along L_m, the chosen mean line of Σ_p.

An additional effective approach for determination of curvatures of generated surface Σ_g is discussed as well. This approach is based on the fact that the normal curvatures and surface torsions (geodesic torsions) of Σ_g are: (i) equal to the normal curvatures and surface torsions of Σ_p along L_m; and (ii) equal to the normal curvatures and surface torsions of tool surface Σ_t along the characteristic L_g (the instantaneous line of tangency of Σ_t and Σ_g).

Mean Line on Ideal Surface Σ_p

The ideal surface Σ_p is considered as a regular one and is represented as

$$\mathbf{r}_p(u_p, \theta_p) \in C^2 \ , \quad \frac{\partial \mathbf{r}_p}{\partial u_p} \times \frac{\partial \mathbf{r}_p}{\partial \theta_p} \neq \mathbf{0} \ , \quad (u_p, \theta_p) \in E \tag{20}$$

where (u_p, θ_p) are the Gaussian coordinates of Σ_p.

The unit normal to Σ_p is represented as

$$\mathbf{n}_p = \frac{\mathbf{N}_p}{|\mathbf{N}_p|}\ , \quad \mathbf{N}_p = \frac{\partial \mathbf{r}_p}{\partial u_p} \times \frac{\partial \mathbf{r}_p}{\partial \theta_p} \tag{21}$$

The determination of mean line on L_m is based on the following procedure:

(i) Initially, we determine numerically n points on surface Σ_p that will belong approximately to the desired mean line L_m.

(ii) Then, we can derive a polynomial function

$$u_{pi}(\theta_{pi}) = \sum_{j=1}^{n} a_j \theta_{pi}^{(n-j)}, \quad (i = 1, ..., n) \tag{22}$$

that will relate surface parameters (u_p, θ_p) for the n points of the mean line on Σ_p.

The mean line L_m, tangent $\mathbf{T}_p$ and unit tangent $\mathbf{t}_p$ to the mean line are represented as follows

$$\mathrm{r}_p(u_p(\theta_p), \theta_p)\ , \quad \mathbf{T}_p = \frac{\partial \mathbf{r}_p}{\partial \theta_p} + \frac{\partial \mathbf{r}_p}{\partial u_p}\frac{du_p}{d\theta_p}\ , \quad \mathbf{t}_p = \frac{\mathbf{T}_p}{|\mathbf{T}_p|} \tag{23}$$

The constraint for $\mathbf{t}_p$ is that it must be of the same sign and differ from zero at the same intervals of interpolation.

Tool Surface

The tool surface Σ_t is represented in coordinate system S_t rigidly connected to the tool by the following equations

$$x_t = x_t(u_t)\cos\theta_t\ , \quad y_t = x_t(u_t)\sin\theta_t\ , \quad z_t = z_t(u_t) \tag{24}$$

The axial section of Σ_t obtained by taking $\theta_t = 0$ represents a circular arc, or a straight line in the case when Σ_t is a circular cone. Surface as shown in equations(24) of the tool is formed by rotation of the axial section of Σ_t about the z_t-axis.

The surface unit normal is determined as

$$\mathbf{n}_t = \frac{\mathbf{N}_t}{|\mathbf{N}_t|}, \quad \mathbf{N}_t = \frac{\partial \mathbf{r}_t}{\partial \theta_t} \times \frac{\partial \mathbf{r}_t}{\partial u_t} \tag{25}$$

Equation of Meshing Between Σ_t and Σ_g

Equation of meshing represents the necessary condition of existence of envelope Σ_g to the family of surfaces Σ_t that is swept out by the tool surface Σ_t.

The equation of meshing can be derived by using the equation

$$\mathbf{N}_i^{(t)} \cdot \mathbf{v}_i^{(tg)} = 0 \tag{26}$$

Here: i indicates the coordinate system Σ_i where the vectors of the scalar product are represented; $\mathbf{N}^{(t)}$ is the normal to surface Σ_t; $\mathbf{v}^{(tg)}$ is the relative velocity in the motion of Σ_t with respect to Σ_g.

Henceforth, we will consider two basic coordinate systems, S_t and S_p, that are rigidly connected to the tool surface Σ_t and the ideal surface Σ_p. In addition to Σ_t, we will consider two trihedrons: $S_b(\mathbf{t}_b, \mathbf{d}_b, \mathbf{n}_b)$ and $S_f(\mathbf{t}_f, \mathbf{d}_f, \mathbf{n}_f)$. Trihedron S_b is rigidly connected to Σ_t and coordinate system S_t (figure 16). Here: O_b is the point of the chosen generatrix of Σ_t where the trihedron is located; $\mathbf{t}_b$ is the tangent to the generatrix at O_b; $\mathbf{n}_b$ is the surface unit normal of Σ_t at O_b; $\mathbf{d}_b = \mathbf{n}_b \times \mathbf{t}_b$; vectors $\mathbf{t}_b$ and $\mathbf{d}_b$ form the tangent plane to Σ_t at O_b. Trihedron S_f moves along the mean line L_m (figure 17); $\mathbf{t}_f$ is the tangent to the mean line L_m at current point M (figure 17); $\mathbf{n}_f$ is the surface unit normal to Σ_p at point M; $\mathbf{d}_f = \mathbf{n}_f \times \mathbf{t}_f$; vectors $\mathbf{t}_f$ and $\mathbf{d}_f$ form the tangent plane to Σ_p at point M.

The tool with surface Σ_t and trihedron S_t moves along mean line L_m of Σ_p and O_b

coincides with current point M of mean line L_m. Surfaces Σ_t and Σ_p are in tangency at any current point M of mean line L_m. The orientation of S_b with respect to S_t is determined with angle β that is varied in the process for generation.

We start the derivations with the case when Σ_t is a circular cone(figure 18). The angular velocity $\boldsymbol{\omega}_f$ of rotation of S_f with respect to S_p is represented as

$$\boldsymbol{\omega}_f = (t\mathbf{t}_f - k_n\mathbf{d}_f + k_g\mathbf{n}_f)\frac{ds}{dt} \tag{27}$$

Here: t is the surface torsion (geodesic torsion), k_n and k_g are the normal and geodesic curvatures of surface Σ_p at current point M of mean line L_m, ds is the infinitesimal displacement along L_m.

The angular velocity $\boldsymbol{\Omega}_f$ of trihedron S_b is represented in S_f as

$$\boldsymbol{\Omega}_f = \boldsymbol{\omega}_f + \frac{d\beta}{dt}\mathbf{n}_f = \begin{bmatrix} t & -k_n & k_g + \frac{d\beta}{ds} \end{bmatrix}^T \frac{ds}{dt} \tag{28}$$

The orientation of cone Σ_t is determined by function $\beta(\theta_p)$ and

$$\frac{d\beta}{ds} = \frac{d\beta}{d\theta_p}\frac{d\theta_p}{ds} = (\frac{d\beta}{d\theta_p})\frac{1}{|\mathbf{T}_p|} \tag{29}$$

where $\mathbf{T}_p$ is the tangent to the mean line L_m at current point M.

The transformations of vector components in transition from S_t to S_b and S_b to S_f are represented by 3×3 matrix operators $\mathbf{L}_{bt}$ and $\mathbf{L}_{fb}$. Here:

$$\mathbf{L}_{fb} = \begin{bmatrix} \cos\beta & -\sin\beta & 0 \\ \sin\beta & \cos\beta & 0 \\ 0 & 0 & 1 \end{bmatrix} \tag{30}$$

$$\mathbf{L}_{bt} = \begin{bmatrix} \sin\gamma_t \cos\theta_t & \sin\gamma_t \sin\theta_t & \cos\gamma_t \\ \sin\theta_t & -\cos\theta_t & 0 \\ \cos\gamma_t \cos\theta_t & \cos\gamma_t \sin\theta_t & -\sin\gamma_t \end{bmatrix} \tag{31}$$

The cone surface Σ_t is represented in S_t as follows (fig. 18)

$$\mathbf{r}_t = u_t \begin{bmatrix} \sin\gamma_t \cos\theta_t & \sin\gamma_t \sin\theta_t & \cos\gamma_t \end{bmatrix}^T \tag{32}$$

where (u_t, θ_t) are the surface parameters, γ_t is the cone apex angle.

The unit normal to the cone surface is

$$\mathbf{n}_t = \begin{bmatrix} \cos\gamma_t \cos\theta_t & \cos\gamma_t \sin\theta_t & -\sin\gamma_t \end{bmatrix}^T \tag{33}$$

The sought-for equation of meshing, necessary condition of existence of envelope Σ_g, is represented in the form:

$$\mathbf{n}_f^{(t)} \cdot \mathbf{v}_f^{(tg)} = 0 \tag{34}$$

where

$$\mathbf{n}_f^{(t)} = \mathbf{L}_{ft}\mathbf{n}_t \tag{35}$$

The derivation of expression $\mathbf{v}_f^{(tg)}$ is simplified while taking into account the following considerations:

(a) The relative velocity vector $\mathbf{v}_f^{(tg)}$ can be represented as

$$\mathbf{v}_f^{(tg)} = \boldsymbol{\Omega}_f^{(s)}\mathbf{r}_f^{(t)} + \frac{ds}{dt}\mathbf{t}_f \tag{36}$$

Here, $\Omega_f^{(s)}$ is the skew-symmetric matrix represented as

$$\Omega_f^{(s)} = \begin{bmatrix} 0 & -\omega_3 & \omega_2 \\ \omega_3 & 0 & -\omega_1 \\ -\omega_2 & \omega_1 & 0 \end{bmatrix} \tag{37}$$

Vector Ω_f is represented by

$$\Omega_f = \omega_1 \mathbf{t}_f + \omega_2 \mathbf{d}_f + \omega_3 \mathbf{n}_f = \begin{bmatrix} t & -k_n & k_g + \frac{d\beta}{ds} \end{bmatrix}^T \frac{ds}{dt} \tag{38}$$

(b) Consider that point N on surface Σ_t(fig. 15) is the point of the characteristic (the line of tangency of Σ_t and the generated surface Σ_g). Certainly, the equation of meshing must be satisfied for point N.

The position vector $\overline{O_f N}$ can be represented as(figs. 15 and 18)

$$\overline{O_f N} = \overline{O_t N} - \overline{O_t O_f} \tag{39}$$

Here, $\overline{O_t N}$ is the position vector of point N that is drawn from the origin O_t of S_t to N; vector $\overline{O_t N}$ is represented in S_t as

$$\overline{O_t N} = u_t \mathbf{e}_t = u_t(\sin\gamma_t \cos\theta_t \ \mathbf{i}_t + \sin\gamma_t \sin\theta_t \ \mathbf{j}_t + \cos\gamma_t \ \mathbf{k}_t) \tag{40}$$

where

$$\mathbf{e}_t = \frac{\frac{\partial}{\partial u_t}(\mathbf{r}_t)}{\left|\frac{\partial}{\partial u_t}(\mathbf{r}_t)\right|} \tag{41}$$

is the unit vector of cone generatrix $\overline{O_t N}$.

Vector $\overline{O_t O_f}$ (figure 18) is represented in S_b as

$$\overline{O_t O_f} = l_t \, \mathbf{i}_b \tag{42}$$

where $l_t = \left|\overline{O_t O_f}\right|$.

Vector $\overline{O_f N}$ is represented in S_f using the matrix equation

$$\mathbf{r}_f^{(t)} = u_t \mathbf{L}_{ft} \mathbf{e}_t - l_t \mathbf{L}_{fb} \mathbf{i}_b \tag{43}$$

(c) We represent now the equation of meshing as

$$\mathbf{n}_f^{(t)} \cdot \mathbf{v}_f^{(ct)} = \mathbf{n}_f^{(t)} \cdot \left[\boldsymbol{\Omega}^{(s)} (u_t \mathbf{L}_{ft} \mathbf{e}_t - l_t \mathbf{L}_{fb} \mathbf{i}_b) \right] + (\mathbf{n}_f^{(t)} \cdot \mathbf{t}_f) \frac{ds}{dt} \tag{44}$$

(d) The further simplification of equation of meshing is based on the following rule for operations with skew-symmetric matrices [5]:

$$\mathbf{A}^T \mathbf{B}^{(s)} \mathbf{A} = \mathbf{C}^{(s)} \tag{45}$$

Here: $\mathbf{B}^{(s)}$ and $\mathbf{C}^{(s)}$ designate skew-symmetric matrices, $\mathbf{A}^T$ is the transpose matrix for $\mathbf{A}$.

Considering that elements of $\mathbf{B}^{(s)}$ are represented in terms of components of vector

$$\mathbf{b} = \begin{bmatrix} b_1 & b_2 & b_3 \end{bmatrix}^T \tag{46}$$

we obtain that the elements of skew-symmetric matrix $\mathbf{C}^{(s)}$ are represented in terms of components of vector $\mathbf{c}$, where

$$\begin{bmatrix} c_1 & c_2 & c_3 \end{bmatrix}^T = \mathbf{A}^T \begin{bmatrix} b_1 & b_2 & b_3 \end{bmatrix}^T \tag{47}$$

Using the above considerations and eliminating $\frac{ds}{dt}$, the final expression of equation of meshing can be represented as

$$\mathbf{n}_f^{(t)} \cdot \mathbf{v}_f^{(tg)} = f(u_t, \theta_t, \theta_p) = u_t \mathbf{n}_t^T \mathbf{A}^{(s)} \mathbf{e}_t - l_t \mathbf{n}_b^T \mathbf{B}^{(s)} \mathbf{i}_b + \mathbf{n}_t^T \mathbf{L}_{ft}^T \mathbf{t}_f = 0 \tag{48}$$

Here:

$$\mathbf{A}^{(s)} \frac{ds}{dt} = \mathbf{L}_{ft}^T \boldsymbol{\Omega}_f^{(s)} \mathbf{L}_{ft} \ , \quad \mathbf{B}^{(s)} \frac{ds}{dt} = \mathbf{L}_{fb}^T \boldsymbol{\Omega}_f^{(s)} \mathbf{L}_{fb} \tag{49}$$

$$\mathbf{A}^{(s)} = \begin{bmatrix} 0 & -a_3 & a_2 \\ a_3 & 0 & -a_1 \\ -a_2 & a_1 & 0 \end{bmatrix} \tag{50}$$

$$\begin{bmatrix} a_1 \\ a_2 \\ a_3 \end{bmatrix} = - \begin{bmatrix} t \cos\beta \sin\gamma_t - k_n \sin\beta \sin\gamma_t + (k_g + \dfrac{d\beta}{ds}) \cos\gamma_t \\ t \sin\beta + k_n \cos\beta \\ t \cos\beta \cos\gamma_t - k_n \sin\beta \cos\gamma_t - (k_g + \dfrac{d\beta}{ds}) \sin\gamma_t \end{bmatrix} \tag{51}$$

$$\mathbf{B}^{(s)} = \begin{bmatrix} 0 & -b_3 & b_2 \\ b_3 & 0 & -b_1 \\ -b_2 & b_1 & 0 \end{bmatrix} \ , \quad \begin{bmatrix} b_1 \\ b_2 \\ b_3 \end{bmatrix} = - \begin{bmatrix} -t \cos\beta + k_n \sin\beta \\ t \sin\beta + k_n \cos\beta \\ -(k_g + \dfrac{d\beta}{ds}) \end{bmatrix} \tag{52}$$

The family of characteristics L_g and the instantaneous lines of tangency of Σ_t and Σ_g are represented in S_t by the equations

$$\mathbf{r}_t = \mathbf{r}_t(u_t, \theta_t) \ , \quad f(u_t, \theta_t, \theta_p) = 0 \tag{53}$$

where θ_p is the parameter of the family of L_g. Taking $\theta_p = \theta_p^{(i)}$ $(i = 1, 2, ..., n)$, we obtain the current characteristics on surface Σ_t.

It is easy to verify that the equation of meshing between Σ_t and Σ_g is satisfied the current point M of mean line L_m on the ideal surface Σ_p. This means that the characteristic L_g intersects L_m at point M, for which we can take $\theta_t = 0$ since Σ_t is a surface of revolution. In the case when Σ_t is a circular cone (figure 18), we can take for point M that $u_t = \left|\overline{O_t O_b}\right| = l_t$.

The approach discussed above for the derivation of the equation of meshing can be easily extended for application in the more general case when the tool surface is a general surface of revolution.

Determination of Generated Surface Σ_g

The ground surface Σ_g is generated as the envelope to the family of tool surface Σ_t; surface Σ_g is represented in S_p by the following equations

$$\mathbf{r}_g^{(p)}(u_p(\theta_p), \theta_p, u_t, \theta_t) = \mathbf{L}_{pf}\mathbf{r}_f^{(t)} + \mathbf{r}_p^{(M)}(u_p(\theta_p), \theta_p) \ , \quad f(u_t, \theta_t, \theta_p) = 0 \tag{54}$$

Here: $f(u_t, \theta_t, \theta_p) = 0$ is the equation of meshing; $\mathbf{r}_f^{(t)}(u_t, \theta_t)$ is the equation of tool surface Σ_t represented in S_f; $\mathbf{r}_p^{(M)}(u_p(\theta_p), \theta_p)$ is the vector function that represents in S_p the mean line L_m; the 3×3 matrix operator $\mathbf{L}_{pf}$ which transforms vectors in transition from S_f to S_p is represented as

$$\mathbf{L}_{pf} = \begin{bmatrix} t_{px} & d_{px} & n_{px} \\ t_{py} & d_{py} & n_{py} \\ t_{pz} & d_{pz} & n_{pz} \end{bmatrix} \tag{55}$$

where

$$\mathbf{t}_p = \frac{\dfrac{\partial}{\partial \theta_p}(\mathbf{r}_p^{(M)})}{\left|\dfrac{\partial}{\partial \theta_p}(\mathbf{r}_p^{(M)})\right|} \tag{56}$$

is the unit tangent to the mean line L_m;

$$\mathbf{n}_p = \pm \frac{\dfrac{\partial \mathbf{r}_p}{\partial u_p} \times \dfrac{\partial \mathbf{r}_p}{\partial \theta_p}}{\left| \dfrac{\partial \mathbf{r}_p}{\partial u_p} \times \dfrac{\partial \mathbf{r}_p}{\partial \theta_p} \right|} \tag{57}$$

$$\mathbf{d}_p = \mathbf{n}_p \times \mathbf{t}_p \tag{58}$$

The sign chosen in equation (57) must provide the direction of $\mathbf{n}_p$ *toward* to the surface of the workpiece under consideration.

Equations (54) represent in S_p the generated surface Σ_g in three-parametric form but with related parameters. Parameter u_t is linear in equation of meshing when Σ_t is a cone, therefore this parameter can be eliminated and the generated surface Σ_g can be represented in S_p as

$$\mathbf{r}_p^{(g)} = \mathbf{r}_g = \mathbf{r}_g(\theta_p, \theta_t) \tag{59}$$

Remember that surfaces Σ_g and Σ_p have a common line L_m where they are in tangency. Surface Σ_g is in tangency with Σ_t along the instantaneous line L_g that passes through current point M of line L_m. The tangents to L_g and L_m lie in the plane that passes through M and is tangent to three surfaces (Σ_p, Σ_g and Σ_t) simultaneously.

Optimal Approximation of Generated Surface Σ_g to Ideal Surface Σ_p

The procedure of optimal approximation of Σ_g to Σ_p is divided into the following stages: (i) design of grid on Σ_p, the net of points, where the deviation of Σ_g from Σ_p will be determined; (ii) determination of initial function $\beta^{(1)}(\theta_p)$ for the first iteration; angle β determines the orientation of the tool surface Σ_t with respect to Σ_p (figures 15 and 17); (iii) determination of deviations of Σ_g from Σ_p with the initial function $\beta^{(1)}(\theta_p)$; (iv) optimal minimization of deviations.

Grid on Surface Σ_p. Figure 19(a) shows the grid on surface Σ_p, the net of (n, m) points,

where the deviations of Σ_g from Σ_p are considered. The position vector is $\overline{O_pQ_{i,j}} = \mathbf{r}_p^{(i,j)}$ (figure 19(b)). The computation is based on the following procedure:

(i) The desired components $L_{i,j}$ and $R_{i,j}$ of the position vector $\mathbf{r}_p^{(i,j)}$ are considered as known.

(ii) Taking into account that

$$L_{i,j} = z_p^{(i,j)} \ , \quad R_{i,j}^2 = [x_p^{(i,j)}(u_p, \theta_p)]^2 + [y_p^{(i,j)}(u_p, \theta_p)]^2 \tag{60}$$

we will obtain the surface Σ_p parameters $(u_p^{(i,j)}, \theta_p^{(i,j)})$ for each grid point.

Determination of Initial Function $\beta^{(1)}$ (θ_p). The determination of $\beta^{(1)}(\theta_p)$ is based on the following idea: the instantaneous direction of $\mathbf{t}_b$ (the tool generatrix) with respect to tangent $\mathbf{t}_f$ to the mean line L_m (figure 17) must provide the minimal value $\left|k_n^{(r)}\right|$. Here: $k_n^{(r)}$ is the relative normal curvature determined as

$$k_n^{(r)} = k_n^{(t)} - k_n^{(p)} \tag{61}$$

where $k_n^{(t)}$ and $k_n^{(p)}$ are the normal curvatures of surfaces Σ_t and Σ_p along $\mathbf{t}_b$. In the case of nondevelopable ruled surface Σ_p, vector $\mathbf{t}_b$ can be directed along the asymptote of Σ_p.

The requirement that $\left|k_n^{(r)}\right|$ is minimal, enables to determine function $\beta^{(1)}(\theta_p)$ numerically. Since we need for further computations the derivative $\dfrac{d\beta}{d\theta_p}$, function $\beta^{(1)}(\theta_p)$ is represented as a polynomial function that must satisfy the numerical data obtained for the chosen points of mean line L_m.

Determination of Deviations of Σ_g from Σ_p. We are able at this stage of investigation to determine the equation of meshing between surfaces Σ_t and Σ_g, and surface Σ_g as discussed above. The computation of deviations of Σ_g from Σ_p at the grid points is based on the following considerations:

(i) Surfaces Σ_p and Σ_g are represented in the same coordinate system (S_p) by the following vector functions:

$$\mathbf{r}_p(u_p, \theta_p) \ , \quad \mathbf{r}_g(\theta_g, \theta_t) \tag{62}$$

(ii) The position vector $\mathbf{r}_p^{(i,j)}$ and surface coordinates $(u_p^{(i,j)}, \theta_p^{(i,j)})$ are known for each point $Q_p^{(i,j)}$ of the grid on surface Σ_p.

(iii) Point $Q_g^{(i,j)}$ on surface Σ_g corresponds to point $Q_p^{(i,j)}$ on surface Σ_p. The surface Σ_g parameters $(\theta_g^{(i,j)}, \theta_t^{(i,j)})$ can be determined by using the following two equations

$$\left.\begin{aligned} y_g^{(i,j)}(\theta_g^{(i,j)}, \theta_t^{(i,j)}) &= y_p^{(i,j)}(u_p^{(i,j)}, \theta_p^{(i,j)}) \\ z_g^{(i,j)}(\theta_g^{(i,j)}, \theta_t^{(i,j)}) &= z_p^{(i,j)}(u_p^{(i,j)}, \theta_p^{(i,j)}) \end{aligned}\right\} \tag{63}$$

(iv) Due to deviations of Σ_g from Σ_p, we have that $x_g^{(i,j)} \neq x_p^{(i,j)}$. The deviation of Σ_g from Σ_p at the grid point $Q_p^{(i,j)}$ is determined by the equation

$$\delta_{i,j} = \mathbf{n}_p^{(i,j)} \cdot (\mathbf{r}_g^{(i,j)} - \mathbf{r}_p^{(i,j)}) \tag{64}$$

where $\mathbf{n}_p^{(i,j)}$ is the unit normal to surface Σ_p at the grid point $Q_p^{(i,j)}$.

The deviation $\delta_{i,j}$ can be positive or negative. We designate as positive such a deviation when $\delta_{i,j} > 0$ considering that $\mathbf{n}_p^{(i,j)}$ is directed into the "body" of surface Σ_p. Positive deviations of Σ_g with respect to Σ_p provide that Σ_g is inside of Σ_p and surface Σ_g is "crowned".

It is not excluded that initially the inequality $\delta_{i,j} > 0$ is not observed yet for all points of the grid. Positive deviations $\delta_{i,j}$ can be provided choosing the following options:

(1) choosing a surface of revolution with a circular arc in the axial section instead of a circular cone; a proper radius of the circular arc must be determined.

(2) changing parameter $l_t = \left|\overline{O_t O_b}\right|$ (figures 17 and 18); this means that the grinding cone will be displaced along $\mathbf{t}_b$ with respect to the mean line L_m.

(3) varying the initially chosen function $\beta^{(1)}(\theta_p)$.

Minimization of Deviations $\delta_{i,j}$. Consider that deviations $\delta_{i,j}$ $(i = 1, ..., n;\ j = 1, ..., m)$ of Σ_g with respect to Σ_p have been determined at the (n, m) grid points. The minimization of deviations can be obtained by corrections of previously obtained function $\beta^{(1)}(\theta_p)$. The correction of angle β is equivalent to the correction of the angle that is formed by the principal directions on surfaces Σ_t and Σ_g. The correction of angle β can be achieved by turning of the tool about the common normal to surfaces Σ_t and Σ_p at their instantaneous point of tangency M_k.

The minimization of deviations $\delta_{i,j}$ is based on the following procedure:

Step 1: Consider the characteristic L_{gk}, the line of contact between surfaces Σ_t and Σ_g, that passes through current point M_k of mean line L_m on surface Σ_p (figure 20). Determine the deviations δ_k between Σ_t and Σ_p along line L_{gk} and find out the maximum deviations designated as $\delta^{(1)}_{kmax}$ and $\delta^{(2)}_{kmax}$. Points of L_{gk} where the deviations are a maximum are designated as $N^{(1)}_k$ and $N^{(2)}_k$. These points are determined in regions I and II of surface Σ_g with line L_m as the border. The simultaneous consideration of the maximum deviations in both regions permits the minimization of the deviations for the whole surface Σ_g.

Note: The deviations of Σ_t from Σ_p along L_{gk} are simultaneously the deviations of Σ_g from Σ_p along L_{gk} since L_{gk} is the line of tangency of Σ_t and Σ_g.

Step 2: The minimization of deviations is accomplished by correction of angle β_k that is determined at point M_k (figure 20). The minimization of deviations is performed locally, for a piece k of surface Σ_g with the characteristic L_{gk}. The process of minimization is a computerized iterative process based on the following considerations:

(i) The objective function is represented as

$$F_k = min(\delta^{(1)}_{kmax} + \delta^{(2)}_{kmax}) \tag{65}$$

with the constraint $\delta_{i,j} \geq 0$.

(ii) The variable of the object function is $\Delta\beta_k$. Then, considering the angle

$$\beta_k^{(2)} = \beta_k^{(1)} + \Delta\beta_k \tag{66}$$

and using the equation of meshing with β_k, we can determine the new characteristic, the piece of envelope $\Sigma_g^{(k)}$ and the new deviations. Iterations are required to provide the sought-for objective function. The final correction of angle β_k we designate as $\beta_k^{(opt)}$.

Note 1: The new contact line $L_{gk}^{(2)}$ (determined with $\beta_k^{(2)}$) slightly differs from the real contact line since the derivative $\frac{d\beta_k^{(1)}}{ds}$ but not $\frac{d\beta_k^{(2)}}{ds}$ is used for determination $L_{gk}^{(2)}$. However, $L_{gk}^{(2)}$ is very close to the real contact line.

Step 3: The procedure discussed must be performed for the set of pieces of surfaces Σ_g with the characteristic L_{gk} for each surface piece. Remember that the deviations for the whole surface must satisfy the inequality $\delta_{i,j} \geq 0$. The procedure of optimization is illustrated with the flowchart shown in figure 21.

Curvatures of Ground Surface Σ_g

The direct determination of curvatures of Σ_g by using surface Σ_g equations is a complicated problem. The solution to this problem can be substantially simplified using the following approach proposed by the authors: (i) the normal curvatures and surface torsions (geodesic torsions) of surfaces Σ_p and Σ_g are equal along line L_m, respectively; (ii) the normal curvatures and surface torsions of surfaces Σ_t and Σ_g are equal along line L_g. This permits the derivation of four equations that represent the principal curvatures of surface Σ_g in terms of normal curvatures and surface torsions of Σ_p and Σ_t. However, only three of these equations are independent (see below).

Further derivations are based on the following equations:

$$k_n = k_I \cos^2 q + k_{II} \sin^2 q = \frac{1}{2}(k_I + k_{II}) + \frac{1}{2}(k_I - k_{II}) \cos 2q \tag{67}$$

$$t = 0.5(k_{II} - k_I)\sin 2q \tag{68}$$

Here: k_I and k_{II} are the surface principal curvatures, angle q is formed by unit vectors $\mathbf{e}_I$ and $\mathbf{e}$ that is measured counterclockwise from $\mathbf{e}_I$ and $\mathbf{e}$; $\mathbf{e}_I$ is the principal direction with principal curvature k_I; $\mathbf{e}$ is the unit vector for the direction where the normal curvature is considered; t is the surface torsion for the direction represented by $\mathbf{e}$.

Equation (67) is known as the Euler equation. Equation (68) is known in the differential geometry as the Bonnet-German equation (see section 5).

The determination of the principal curvatures and principal directions for Σ_g is based on the following computational procedure (see section 5):

Step 1: Determination of $k_n^{(1)}$ and $t^{(1)}$ for surface Σ_g at the direction determined by the tangent to L_m.

The determination is based on equations (67) and (68) applied for surface Σ_p. Recall that Σ_p and Σ_g have the same values of $k_n^{(1)}$ and $t^{(1)}$ along the above mentioned direction.

Step 2: Determination of $k_n^{(2)}$ and $t^{(2)}$.

The designations $k_n^{(2)}$ and $t^{(2)}$ indicate the normal curvatures of Σ_g and the surface torsion along the tangent to L_g. Recall that $k_n^{(2)}$ and $t^{(2)}$ are the same for Σ_t and Σ_g along L_g. We determine $k_n^{(2)}$ and $t^{(2)}$ for surface Σ_t using equations (67) and (68), respectively.

Step 3: We consider at this stage of computation that for surface Σ_g are known: $k_n^{(1)}$ and $t^{(1)}$, $k_n^{(2)}$ and $t^{(2)}$, for two directions with tangents $\boldsymbol{\tau}_1$ and $\boldsymbol{\tau}_2$ that form the known angle μ (fig. 22). Our goal is to determine angle q_1 (or q_2) for the principal direction $\mathbf{e}_I^{(g)}$ and the principal curvatures $k_I^{(g)}$ and $k_{II}^{(g)}$ (figure 22).

Using equations (67) and (68), we can prove that $k_n^{(i)}$ and $t^{(i)}$ $(i = 1, 2)$ given for two directions represented by $\boldsymbol{\tau}_1$ and $\boldsymbol{\tau}_2$ are related with the following equation

$$\frac{t^{(1)} + t^{(2)}}{k_n^{(2)} - k_n^{(1)}} = \cot\mu \tag{69}$$

Step 4: Using equations (67) and (68), we can derive the following three equations for determination of q_1, $k_I^{(g)}$ and $k_{II}^{(g)}$

$$\tan 2q_1 = \frac{t^{(1)} \sin 2\mu}{t^{(2)} - t^{(1)} \cos 2\mu} \tag{70}$$

$$k_I^{(g)} = k_n^{(1)} - t^{(1)} \tan q_1 \tag{71}$$

$$k_{II}^{(g)} = k_n^{(1)} + t^{(1)} \cot q_1 \tag{72}$$

Equation (70) provides two solutions for q_1 ($q_1^{(2)} = q_1^{(1)} + 90°$) and both are correct. We choose the solution with the smaller value of q_1.

Numerical Example 1: Grinding of Archimedes' Worm Surface

The worm surface shown in figure 23 is a ruled undeveloped surface formed by the screw motion of straight line $\overline{KN}$ ($|\overline{KN}| = u_p$). The screw motion is performed in coordinate system S_p (figure 23(b)). The to be ground surface Σ_p is represented in S_p as

$$r_p = u_p \cos\alpha \cos\theta_p \, \mathbf{i}_p + u_p \cos\alpha \sin\theta_p \, \mathbf{j}_p + (p\theta_p - u_p \sin\alpha) \, \mathbf{k}_p \tag{73}$$

where u_p and θ_p are the surface parameters.

The surface unit normal is

$$\mathbf{n}_p = \frac{\mathbf{N}_p}{|\mathbf{N}_p|}, \quad \mathbf{N}_p = \frac{\partial \mathbf{r}_p}{\partial u_p} \times \frac{\partial \mathbf{r}_p}{\partial \theta_p} \tag{74}$$

Thus:

$$\mathbf{n}_p = \frac{1}{(u_p^2 + p^2)^{0.5}} \begin{bmatrix} p\sin\theta_p + u_p \sin\alpha\cos\theta_p \\ -p\cos\theta_p + u_p \sin\alpha\sin\theta_p \\ u_p\cos\alpha \end{bmatrix} \qquad \text{(provided} \quad \cos\alpha \neq 0) \qquad (75)$$

As an example the following data will be used:

Number of threads, N_1,	=	2
Axial diametral pitch, P_{ax},	=	$8\ (\frac{1}{\text{in}})$
α	=	$20°$
The radius of the pitch cylinder	=	$1.125\ (in)$

(i) The screw parameter is

$$p = \frac{N_1}{2P_{ax}} = 0.125 \text{ in.}$$

(ii) The lead angle is

$$\tan\lambda_p = \frac{p}{r_p} = \frac{0.125}{1.25}\ , \quad \lambda_p = 5.7106°$$

The mean line is determined as

$$\mathbf{r}_p(u_m, \theta_p)\ , \quad u_m = \frac{\left(r_p + \frac{1}{P_{ax}}\right) + \left(r_p - \frac{1.25}{P_{ax}}\right)}{2\cos\alpha} = \frac{r_p - \frac{0.125}{P_{ax}}}{\cos\alpha} = 1.3136 \text{ in.}$$

where $\frac{1}{P_{ax}}$ and $\frac{1.25}{P_{ax}}$ determine the addendum and dedendum of the worm.

The worm is ground by a cone with the apex angle $\gamma_t = 30°$, and outside diameter 8 in..

The inside angle $\beta^{(1)} = -88.0121°$ provides the coincidence of both generatrices of the cone and the Archimedes' worm. The maximal deviation of the ground surface Σ_g from the

ideal surface Σ_p with the above value of $\beta^{(1)}$ is 3 microns.

The optimal angle $\beta^{(opt)} = -94.6788°$ has been determined by the optimization method developed. The deviations of the ground surface Σ_g from Σ_p with the optimal $\beta^{(opt)}$ are positive and the maximal deviation has been reduced to 0.35 microns(figure 24).

5. Condensed Information About Surface Curvature

The contents of this section provide a condensed overview of about the basic equations of surface curvatures. For further explanation of the details please refer to the books by Nutbourne and Martin[6], Favard[7] and Litvin[2].

Osculating Plane

Figure 25 shows spatial curve L_1ML_2. The *osculating* plane is the limiting position of such a plane that passes through curve points M_1, M, and M_2 as M_1 and M_2 approach M.

The osculating plane for a curve at its regular point M is formed by the *tangent* to the curve and the *acceleration* vector for the same point.

The osculating plane and the curve are in tangency of *second* order. The osculating plane is an exceptional tangent plane. The deviations of the curve from the osculating plane are of different signs on the two sides from the point of tangency, and the curve is above and below the plane (see points L_1 and L_2 in figure 25). An exception is the case when the point of tangency is a *rectification* point at which the second derivative $\mathbf{r}_{ss}$ of a curve represented by $\mathbf{r}(s)$ is equal to zero. Here: s is the arc length of the curve.

Space Curve and Surface Trihedron

Henceforth, we will consider two trihedrons, the space curve trihedron and the surface trihedron. Each of the trihedrons is right-handed, formed by three mutually perpendicular vectors. The concept of space curve trihedron is discussed when a space curve is considered in the 3D space and the curve is not related to a surface. The concept of surface trihedron

and space curve trihedron are considered simultaneously when the space curve belongs to a certain surface and the curve inherits some of the properties of the surface to which it belongs.

Space Curve Trihedron

We consider a coordinate system that is rigidly connected to the curve. Position vector $\overline{OC} = \mathbf{r}(s)$ determines the *current* point C of the curve (figure 25); $s = \overset{\frown}{MC}$ is the length of the curve arc; M is the *starting* point.

Consider that a small piece of curve L_1ML_2 is located in the osculating plane Π_o(figure 25). Plane Π_N is perpendicular to plane Π_o and passes through point M of the curve.

We define the normal **N** to the curve as a vector that is perpendicular to the tangent to the curve. There is an infinite number of normals **N** to the curve at its point M. All of normals **N** belong to plane Π_N since the unit tangent **t** is perpendicular to Π_N. For instance, vector $\mathbf{N}_i$ is one of the set of curve normals(figure 25). Two normals of the set of normals must be specified:

(i) the *principal* normal with the unit vector **m** that lies in the osculating plane Π_o and is the line of intersection of planes Π_o and Π_N (figure 25) and

(ii) the *binormal* **b** that is perpendicular to **t** and **m** simultaneously.

We may identify at each *current* point of the curve three mutually orthogonal vectors (figure 25): the *tangent* vector **t**, the *principal normal* **m**, and the *binormal* **b**. The orientation of these vectors in a fixed coordinate system is varied, depending on the location of the point on the curve. We may consider now a trihedron S_c as a rigid body with three mutually perpendicular vectors $\mathbf{e}_c(\mathbf{i}_c, \mathbf{j}_c, \mathbf{k}_c)$ that form a right trihedron (figure 26). The origin of the trihedron moves along the curve, and the unit vectors $\mathbf{i}_c$, $\mathbf{j}_c$, $\mathbf{k}_c$ represent **t**, **m**, **b**, respectively. Unit vectors **t**, **m**, **b** are taken at the current point of the curve where the origin of trihedron S_c is located at this instant.

The representation of unit vectors **t**, **m**, and **b** in terms of derivatives of vector function

$\mathbf{r}(s)$ is based on the following consideration:

(i) Unit vectors $\mathbf{t}$, $\mathbf{m}$, and $\mathbf{b}$ form a right-hand trihedron (figures 25 and 26). Thus

$$\mathbf{t} = \mathbf{m} \times \mathbf{b}\ , \quad \mathbf{m} = \mathbf{b} \times \mathbf{t}, \quad \mathbf{b} = \mathbf{t} \times \mathbf{m} \tag{76}$$

(ii) Unit vector $\mathbf{t}$ is directed along the tangent to the curve and therefore

$$\mathbf{t}(s) = \frac{d\mathbf{r}}{ds} = \mathbf{r}_s$$

Vector $\mathbf{r}_s$ is a unit vector since $\mid d\mathbf{r} \mid = ds$.

(iii) The principal normal to the curve is perpendicular to the curve tangent $\mathbf{t} = \mathbf{r}_s$. The derivative $\mathbf{r}_{ss} = \frac{d}{ds}(\mathbf{r}_s)$ is perpendicular to $\mathbf{r}_s$, lies in the osculating plane and therefore the unit vector $\mathbf{m}$ of the principal normal is represented as

$$\mathbf{m}(s) = \frac{\mathbf{r}_{ss}}{\mid \mathbf{r}_{ss} \mid}$$

(iv) Taking into account the expression for $\mathbf{b}$ in equations (76), we obtain the following equation for the binormal

$$\mathbf{b}(s) = \mathbf{t} \times \mathbf{m} = \frac{\mathbf{r}_s \times \mathbf{r}_{ss}}{\mid \mathbf{r}_{ss} \mid}$$

Frenet-Serret Equations

The motion of the trihedren along a spatial curve can be represented in two components: (i) as a translational motion along the curve (the origin of the trihedron moves along the curve

and the unit vectors of the trihedron keep their original orientation), (ii) and as a rotational motion (the trihedron is rotated as a rigid body (to be coincided with the principal normal $\mathbf{m}_c$ and the tangent $\mathbf{t}_c$ to the curve at the curve neighboring point).

Consider that the origin of curve trihedron coincides with point M of the curve and the unit vectors $\mathbf{t}_c$, $\mathbf{m}_c$ and $\mathbf{b}_c$ determine the instantaneous orientation of the trihedron(figure 26). The neighboring point of the curve is N and $|\overline{MN}| = ds$,where s is the arc length of the curve. The unit vectors of the trihedron at N are determined as ($\mathbf{t}_c^*$, $\mathbf{m}_c^*$ and $\mathbf{b}_c^*$), where

$$\mathbf{t}_c^* = \mathbf{t}_c + \mathbf{t}_{sc}ds, \quad \mathbf{m}_c^* = \mathbf{m}_c + \mathbf{m}_{sc}ds, \quad \mathbf{b}_c^* = \mathbf{b}_c + \mathbf{b}_{sc}ds \tag{77}$$

Here:

$$\mathbf{t}_{sc} = \frac{d\mathbf{t}_c}{ds}, \quad \mathbf{m}_{sc} = \frac{d\mathbf{m}_c}{ds}, \quad \mathbf{b}_{sc} = \frac{d\mathbf{b}_c}{ds} \tag{78}$$

that are taken at point M.

Frenet-Serret equations define $\mathbf{t}_{sc}$, $\mathbf{m}_{sc}$ and $\mathbf{b}_{sc}$ as follows (see References [6], [7] and [2]):

$$\begin{bmatrix} \mathbf{t}_{sc} \\ \mathbf{m}_{sc} \\ \mathbf{b}_{sc} \end{bmatrix} = \begin{bmatrix} \kappa_o \mathbf{m}_c \\ \tau \mathbf{b}_c - \kappa_o \mathbf{t}_c \\ -\tau \mathbf{m}_c \end{bmatrix} = \begin{bmatrix} 0 & \kappa_o & 0 \\ -\kappa_o & 0 & \tau \\ 0 & -\tau & 0 \end{bmatrix} \begin{bmatrix} \mathbf{t}_c \\ \mathbf{m}_c \\ \mathbf{b}_c \end{bmatrix} \tag{79}$$

where κ_o and τ are the curvature and torsion of the space curve at point M. It is evident that in the case of a planar curve, the unit vector $\mathbf{b}_c$ is perpendicular to the plane where the

curve is located, $\mathbf{b}_{sc}$ is equal to zero and the curve torsion τ of a planar curve is equal to zero.

Equations of κ_o and τ for a Parametric Spatial Curve

Consider that the spatial curve is represented by vector function $\mathbf{r}(\theta)$. After derivations we obtain (see References [2], [6], and [7])

$$\begin{aligned} \kappa_o &= \frac{\mathbf{r}_{\theta\theta} \cdot \mathbf{m}}{\mathbf{r}_\theta^2} = \frac{|\, \mathbf{r}_\theta \times \mathbf{r}_{\theta\theta} \,|}{|\, \mathbf{r}_\theta \,|^3} \\ &= \frac{[(x_\theta y_{\theta\theta} - x_{\theta\theta} y_\theta)^2 + (x_\theta z_{\theta\theta} - x_{\theta\theta} z_\theta)^2 + (y_\theta z_{\theta\theta} - y_{\theta\theta} z_\theta)^2]^{1/2}}{(x_\theta^2 + y_\theta^2 + z_\theta^2)^{3/2}} \end{aligned} \tag{80}$$

The curvature κ_o obtained from equation (80) is always positive because the principal normal $\mathbf{m}_c$ is located in the osculating plane and is directed to the center of curve curvature.

The curve curvature κ_o can be also represented in the form

$$\kappa_o = \frac{\mathbf{a}_\tau \cdot \mathbf{m}}{\mathbf{v}_\tau^2} \tag{81}$$

Here: $\mathbf{v}_\tau$ and $\mathbf{a}_\tau$ are the velocity and acceleration of a point in its motion along the curve and are represented as follows

$$\mathbf{v}_\tau = \mathbf{r}_\theta \frac{d\theta}{dt} \tag{82}$$

$$\mathbf{a}_\tau = \mathbf{r}_{\theta\theta} \left(\frac{d\theta}{dt}\right)^2 + \mathbf{r}_\theta \left(\frac{d^2\theta}{dt^2}\right) \tag{83}$$

Obviously, the curvature κ_o can be also represented as

$$\kappa_o = \frac{\mathbf{r}_{\theta\theta} \cdot \mathbf{m}}{\mathbf{r}_\theta^2} \tag{84}$$

The space curve torsion τ is represented by the equation

$$\tau(\theta) = \frac{(\mathbf{r}_\theta \times \mathbf{r}_{\theta\theta}) \cdot \mathbf{r}_{\theta\theta\theta}}{(\mathbf{r}_\theta \times \mathbf{r}_{\theta\theta})^2} \tag{85}$$

In the case of a planar curve, we have $(\mathbf{r}_\theta \times \mathbf{r}_{\theta\theta}) \cdot \mathbf{r}_{\theta\theta\theta} = 0$ and $\tau = 0$.

Surface Curve Trihedron

Consider a regular surface Σ that is represented by

$$\mathbf{r}(u, \theta) \in C^2 \ , \quad \mathbf{r}_u \times \mathbf{r}_\theta \neq 0 \ , \quad (u, \theta) \in A \tag{86}$$

A curve on Σ is determined if in vector function $\mathbf{r}(u, \theta)$ surface parameters are related with the equation

$$f(u, \theta) = 0 \ , \qquad f_u^2 + f_\theta^2 \neq 0 \tag{87}$$

Figure 27 shows two curves, L_n and L_o, that pass through the *same* surface point M and have the *same* tangent. Curve L_n is a planar curve obtained by intersection of the surface by the surface normal plane that is drawn through the unit tangent $\mathbf{t}$ and the surface unit normal $\mathbf{n}$. Curve L_o is a spatial curve identified *locally* with the orientation of osculating plane, the curvature and the torsion of the curve. Considering that a spatial curve belongs to a surface, we may determine more parameters for the local identification of the curve.

We have introduced in above the curve trihedron $S_c(\mathbf{i}_c,\ \mathbf{j}_c,\ \mathbf{k}_c)$ where $\mathbf{i}_c = \mathbf{t}$ is the unit tangent, $\mathbf{j}_c = \mathbf{m}$ is the curve principal normal, and $\mathbf{k}_c = \mathbf{b}$ is the curve binormal (figures 26 and 27(b)). In addition, we set up now the surface trihedron $S_f(\mathbf{i}_f,\ \mathbf{j}_f,\ \mathbf{k}_f)$ shown in figure 27(b). Here: $\mathbf{i}_f = \mathbf{t}$ is the unit tangent to the spatial curve, $\mathbf{j}_f = \mathbf{d}$ is the unit vector that is perpendicular to $\mathbf{t}$ and lies in the plane tangent to the surface at point M; $\mathbf{k}_f = \mathbf{n}$ is the surface unit normal. Subscript "f" indicates that the surface trihedron and its axes are considered.

The unit tangent $\mathbf{i}_f = \mathbf{i}_c = \mathbf{t}$ is determined as

$$\mathbf{t} = \frac{\mathbf{T}}{|\,\mathbf{T}\,|}\,, \quad \mathbf{T} = \mathbf{r}_u + \mathbf{r}_\theta \frac{d\theta}{du} = \mathbf{r}_u - \mathbf{r}_\theta \frac{f_u}{f_\theta} \qquad (f_\theta \neq 0) \tag{88}$$

The surface unit normal is represented as

$$\mathbf{n} = \frac{\mathbf{N}}{|\,\mathbf{N}\,|}\,, \quad \mathbf{N} = \mathbf{r}_u \times \mathbf{r}_\theta \qquad (\mathbf{n} = \mathbf{k}_f) \tag{89}$$

Changing the order in the cross product in equation (89), we can change the direction of $\mathbf{n}$ for the opposite one, and provide $\delta < 90°$, where δ is formed by $\mathbf{n}$ and $\mathbf{m}$. We remind that the direction of $\mathbf{m}$ is the same as $\mathbf{r}_{ss}$ (assuming that the curve is represented by $\mathbf{r}(s)$) and cannot be chosen arbitrarily. Unit vectors $\mathbf{t}$, $\mathbf{d}$, and $\mathbf{n}$ form the right trihedron S_f, the surface trihedron.

Bonnet-Kovalevski Equations

Figure. 27(b) shows the curve and surface trihedrons whose common origin is located at the current point M of spatial curve L_o. Consider now that the common origin of both trihedrons is moved along L_o to the neighboring point N. Both trihedrons will keep the tangent $\mathbf{t}^*$ to L_o at point N as their common axis, but one of the trihedrons will be turned

with respect to the other one since the motion along L_o will be accompanied with the change of angle δ formed by vector $\mathbf{m}$ and $\mathbf{n}$. Obviously, the unit vectors of the surface trihedron will change at N their orientation with respect to the orientation at M. Designating the unit vectors at N by $\mathbf{t}^*$, $\mathbf{d}^*$ and $\mathbf{n}^*$, we have

$$\mathbf{t}^* = \mathbf{t}(s) + \mathbf{t}_s ds, \quad \mathbf{d}^* = \mathbf{d}(s) + \mathbf{d}_s ds, \quad \mathbf{n}^* = \mathbf{n}(s) + \mathbf{n}_s ds \tag{90}$$

where

$$\mathbf{t}_s = \frac{d}{ds}(\mathbf{t}(s)), \quad \mathbf{d}_s = \frac{d}{ds}(\mathbf{d}(s)), \quad \mathbf{n}_s = \frac{d}{ds}(\mathbf{n}(s)) \tag{91}$$

Bonnet-Kovalevski equations express the derivatives $\mathbf{t}_s$, $\mathbf{d}_s$ and $\mathbf{n}_s$ in terms of κ_g, κ_n and t as follows (see References [6] and [2]).

$$\left.\begin{aligned} \mathbf{t}_s &= \kappa_g \mathbf{d} + \kappa_n \mathbf{n} = \kappa_g \mathbf{j}_f + \kappa_n \mathbf{k}_f \\ \mathbf{d}_s &= -\kappa_g \mathbf{t} + t\mathbf{n} = -\kappa_g \mathbf{i}_f + t\mathbf{k}_f \\ \mathbf{n}_s &= -\kappa_n \mathbf{t} - t\mathbf{d} = -\kappa_n \mathbf{i}_f - t\mathbf{j}_f \end{aligned}\right\} \tag{92}$$

Here: κ_n, κ_g and t are the surface normal curvature, geodesic curvature, and the surface torsion, respectively. The concept of surface normal and principal curvatures is discussed in many books on differential geometry, but the determination and concept of κ_g and t requires additional explanation that is presented next in this report.

Geodesic Curvature

Frenet-Serret equations (92) yield that

$$\mathbf{t}_s = \kappa_o \mathbf{m} \tag{93}$$

where κ_o is the curvature of a spatial curve; the curvature center lies in the osculating plane. Equations (92) and (93) yield that

$$\kappa_o \mathbf{m} = \kappa_g \mathbf{d} + \kappa_n \mathbf{n} \tag{94}$$

Equation (94) can be interpreted follows:

(1) Figure 29 shows a spatial curve L_o on surface Σ. Unit vectors $\mathbf{t}$, $\mathbf{d}$, and $\mathbf{n}$ represent the surface trihedron (figures 29 and 27(b)). Here: $\mathbf{t}$ is the tangent to curve L_o; $\mathbf{d}$ lies in the tangent plane and is perpendicular to $\mathbf{t}$; $\mathbf{n}$ is the surface unit normal. Unit vector $\mathbf{m}$ is the principal normal to L_o and lies in the osculating plane. Vector $\mathbf{r}_{ss} = \kappa_o \mathbf{m}$.

(2) Consider now that the spatial curve L_o is projected on the tangent plane T and normal plane N, respectively. The projections are designated by L_T and L_N. We emphasize that there is no difference between L_N (figure 29(b)) and L_n (figure 28) if they are considered locally. Both curves have the same normal curvature at the point of tangency M.

(3) Vector $\kappa_o \mathbf{m}$ is represented as the sum of two vectors: $\kappa_g \mathbf{d}$ and $\kappa_n \mathbf{n}$. The scalar κ_g represents the curvature of curve L_T, and the scalar κ_n represents the curvature of curve L_n.

(4) Equation (94) yields two relations

$$\kappa_o(\mathbf{m} \cdot \mathbf{n}) = \kappa_o \cos\delta = \kappa_n \tag{95}$$

$$\kappa_g = \mathbf{r}_{ss} \cdot \mathbf{d} = \kappa_o \sin\delta \tag{96}$$

where δ is the angle formed by vectors $\mathbf{m}$ and $\mathbf{n}$ that determines the orientation of osculating plane with respect to the normal plane. Equations (95) and (96) relate curvatures κ_o and κ_n and angle δ.

The direct determination of geodesic curvature of a spatial curve represented on a surface is based on the following equations:

(i) Consider that the surface is represented by the vector function $\mathbf{r}(u, \theta)$.

(ii) A spatial curve is represented on the surface as

$$\mathbf{r}(u(\theta), \theta) \tag{97}$$

where $u(\theta)$ is the known function.

(iii) The tangent to the curve is represented as

$$\mathbf{T} = \mathbf{r}_u \frac{du}{d\theta} + \mathbf{r}_\theta \tag{98}$$

(iv) The unit normal to the surface is represented as

$$\mathbf{n} = \frac{\mathbf{N}}{|\,\mathbf{N}\,|}, \quad \mathbf{N} = \mathbf{r}_u \times \mathbf{r}_\theta \tag{99}$$

(v) An auxiliary parameter $\mathbf{a}$ is represented as

$$\mathbf{a} = \mathbf{r}_{uu}(\frac{du}{d\theta})^2 + 2\mathbf{r}_{u\theta}\frac{du}{d\theta} + \mathbf{r}_{\theta\theta} \tag{100}$$

(vi) The final expression for κ_g is

$$\kappa_g = \frac{\mathbf{T} \cdot (\mathbf{a} \times \mathbf{n}) - \mid \mathbf{N} \mid \frac{d^2u}{d\theta^2}}{\mid \mathbf{T} \mid^3} \tag{101}$$

Surface Torsion

The surface torsion t can be represented by the equation

$$t = \tau + \delta_s = \tau + \frac{d}{ds}(\delta) \tag{102}$$

Thus, the surface torsion depends on the torsion τ of the spatial curve along which the origin of two trihedrons is moved, and on the derivative δ_s where δ is the angle formed by the unit vectors **m** and **n** of the trihedrons.

The geometric interpretation of the surface torsion may be based on the concept of the *geodesic line* (see References [6] and [2]). A spatial line on the surface is the geodesic one if the principal normal **m** at any curve point M coincides with the surface normal at M. The geodesic curvature of the geodesic line at any curve point is equal to zero.

It was proven in differential geometry that the surface torsion t is the curve torsion of the geodesic line.

A simple method for computation of the surface torsion is based on the equation that has been proposed by Sophia Germain and Bonnet (see References [6], [2] and [7]). This equation is

$$t = 0.5(\kappa_{II} - \kappa_I) \sin 2q \tag{103}$$

Here: κ_I and κ_{II} are the principal curvatures of the surface at point M on the principal directions with the unit vectors $\mathbf{e}_I$ and $\mathbf{e}_{II}$(fig. 30); q is the angle formed by $\mathbf{e}_I$ and **t**.

Using equation (103) and Euler's equations that relate the principal curvatures and normal curvatures, we may determine the solutions to the following two problems (Ref. [2]):

Problem 1: Consider that two directions in the tangent plane determined with unit vectors $\mathbf{t}^{(1)}$ and $\mathbf{t}^{(2)}$ are given (figure 31). The angle μ formed by $\mathbf{t}^{(1)}$ and $\mathbf{t}^{(2)}$ is known. Also the following are known: (i) the normal curvatures $\kappa_n^{(1)}$ and $\kappa_n^{(2)}$ for directions of $\mathbf{t}^{(1)}$ and $\mathbf{t}^{(2)}$, and (ii) the surface torsion $t^{(1)}$ given for direction $\mathbf{t}^{(1)}$.

The goal is to determine the principal curvatures κ_I and κ_{II} for directions of $\mathbf{t}^{(1)}$ and $\mathbf{t}^{(2)}$, and angle $q^{(1)}$ (or $q^{(2)}$).

The solution to this problem is represented by the following equations [2]

$$\tan 2q^{(1)} = \frac{t^{(1)}(1-\cos 2\mu)}{\kappa_n^{(2)} - \kappa_n^{(1)} - t^{(1)} \sin 2\mu} \tag{104}$$

$$\kappa_I = \kappa_n^{(1)} - t^{(1)} \tan q^{(1)} \tag{105}$$

$$\kappa_{II} = \kappa_n^{(1)} + t^{(1)} \cot q^{(1)} \tag{106}$$

Problem 2: Consider as given $\mathbf{t}^{(1)}$, $\mathbf{t}^{(2)}$ (figure 31), $\kappa_n^{(1)}$ and $\kappa_n^{(2)}$. The goal is to relate the surface torsions for directions of $\mathbf{t}^{(1)}$ and $\mathbf{t}^{(2)}$.

The sought-for relation is represented by the equation [2]

$$\frac{t^{(1)} + t^{(2)}}{\kappa_n^{(2)} - \kappa_n^{(1)}} - \cot \mu = 0 \tag{107}$$

where μ is the angle formed by $\mathbf{t}^{(1)}$ and $\mathbf{t}^{(2)}$.

Numerical Example 2: Determination of the geodesic curvature κ_g and surface torsion t of Archimede's worm surface

Archimede's worm surface is represented as

$$\mathbf{r} = \begin{bmatrix} u\cos\alpha\cos\theta \\ u\cos\alpha\sin\theta \\ p\theta - u\sin\alpha \end{bmatrix} \tag{108}$$

Here u and θ are the Gaussian coordinates, α is the pressure angle and p is the screw parameter. A helix on the Archimede's worm surface is a spatial curve obtained by intersection of the worm surface by a cylinder of radius r_i. Our goal is to determine the geodesic curvature κ_g of the helix and the surface torsion of the Archemede's worm surface.

(1) Geodesic curvature κ_g

Taking into account the $r_x^2 + r_y^2 = r_i^2$, we can represent the helix as follows

$$u = \frac{r_i}{\cos\alpha}, \quad \mathbf{r}(\theta) = \begin{bmatrix} r_i\cos\theta \\ r_i\sin\theta \\ p\theta - r_i\tan\alpha \end{bmatrix} \tag{109}$$

The tangent to the helix can be represented as

$$\mathbf{T} = \frac{\partial \mathbf{r}}{\partial \theta} = (-r_i\sin\theta \quad r_i\cos\theta \quad p)^T \tag{110}$$

The unit surface normal is represented by equations (99) and (75)

$$\mathbf{n} = \frac{1}{\sqrt{p^2 + u^2}} \begin{bmatrix} p\sin\theta + u\sin\alpha\cos\theta \\ -p\cos\theta + u\sin\alpha\sin\theta \\ u\cos\alpha \end{bmatrix} \tag{111}$$

The auxiliary vector **a** is (see equation (100))

$$\mathbf{a} = (-r_i\cos\theta \quad -r_i\sin\theta \quad 0)^T \tag{112}$$

Equations (101) and (110) to (112) yield the following expression for the geodesic curvature

$$\kappa_g = \frac{\mathbf{T}\cdot(\mathbf{a}\times\mathbf{n})}{|\mathbf{T}|^3} = \frac{r_i\cos\alpha}{\sqrt{(p^2 + r_i^2)(p^2\cos^2\alpha + r_i^2)}} \tag{113}$$

(2) Surface torsion t

From Reference [2] (F. L. Litvin, 1993), the principal curvatures and principal directions at a surface point can be represented by the following equations:

$$\kappa_i = \frac{Lh_i + M}{Eh_i + F}, \quad (i = I, II) \tag{114}$$

$$\mathbf{e}_i = \frac{\mathbf{r}_u h_i + \mathbf{r}_\theta}{|\mathbf{r}_u h_i + \mathbf{r}_\theta|} \quad (i = I, II) \tag{115}$$

The coefficients and the partial derivative in the case of the Archimedes' worm can be expressed as follows:

$$L = 0, \quad M = -\frac{p\cos\alpha}{(u^2+p^2)^{\frac{1}{2}}}, \quad F = -p\sin\alpha, \quad E = 1 \tag{116}$$

$$h_i = \frac{-u^2\sin\alpha \pm (u^4\sin^2\alpha + 4p^2u^2 + 4p^4)^{\frac{1}{2}}}{2p}, \quad (i = I, II) \tag{117}$$

$$\mathbf{r}_u = (\cos\alpha\cos\theta \quad \cos\alpha\sin\theta \quad -\sin\alpha)^T \tag{118}$$

$$\mathbf{r}_\theta = \frac{1}{\sqrt{p^2+u^2\cos^2\alpha}}(-u\cos\alpha\sin\theta \quad u\cos\alpha\cos\theta \quad p)^T \tag{119}$$

Angle q that is formed by tangent $\mathbf{T}$ and $\mathbf{e}_I$ is

$$q = \cos^{-1}(\frac{\mathbf{e}_I \cdot \mathbf{T}}{|\mathbf{T}|}) \tag{120}$$

Considering that κ_I, κ_{II} and angle q are given, we can obtain the surface torsion along the tangent $\mathbf{T}$ as

$$t = 0.5(\kappa_{II} - \kappa_I)\sin 2q \tag{121}$$

(3) Computation results

The to be computed point is located on the helix that belongs to the pitch cylinder of the worm. The z-coordinate of the helix point is equal to zero, and the Gaussian coordinates are

$$u = \frac{r_p}{\cos\alpha}, \quad \theta = \frac{r_p}{p}\tan\alpha$$

The design parameters are the same as in Numerical Example 1, i.e.

$$r_p = 1.25in, \quad p = 0.125in, \quad \alpha = 20^\circ$$

The results of computation are

$$\kappa_g = 0.8257\frac{1}{in}, \quad t = -0.1540\frac{1}{in}, \quad \kappa_I = -0.3283\frac{1}{in}, \quad \kappa_{II} = 0.0227\frac{1}{in}$$

6. Conclusion

From the analytical study presented in this report the following conclusions can be drawn:

(1) The kinematics of two CNC machines with 6 degrees-of-freedom has been described.

(2) The preliminary results of investigation by TCA of the sensitivity of helical gears and worm-gear drives to misalignment are represented.

(3) A new method for grinding of a gear tooth surface with optimal approximation to the given surface is proposed.

(4) An algorithm for the execution of motions of a CNC machine for the surface generation has been developed.

References

1 Litvin F. L., N. X. Chen, Y. Zhang, T. J. Krenzer and R. F. Handschuh, "Computerized Generation of Surfaces with Optimal Approximation to Ideal Surface," Computer Methods in Applied Mechanics and Engineering, will be published soon, 1993.

2 Litvin F. L., Gear Geometry and Applied Theory, Prentice Hall, 1993, in Press.

3 Litvin F. L., Zhang J., Handschuh R. F. and Coy J. J., Topology of Modified Helical Gears, J. Surface Topography, March 1989, vol. 2, Issue 1, pp. 41-58.

4 Goldrich, Robert N., "Theory of 6-Axis CNC Generation of Spiral Bevel and Hypoid Gears," AGMA paper 89FTM9, 1989.

5 Litvin F. L., Theory of Gearing, NASA Reference Publication 1212, 1989.

6 Nutbourne A. W. and Martin R. R., Differential Geometry Applied to Curve and Surface Design, vol.1, Ellis Horwood Limited, 1953.

7 Favard, J., Course of Local Differential Geometry, Gauthier-Villars, (in French and translated into Russian).

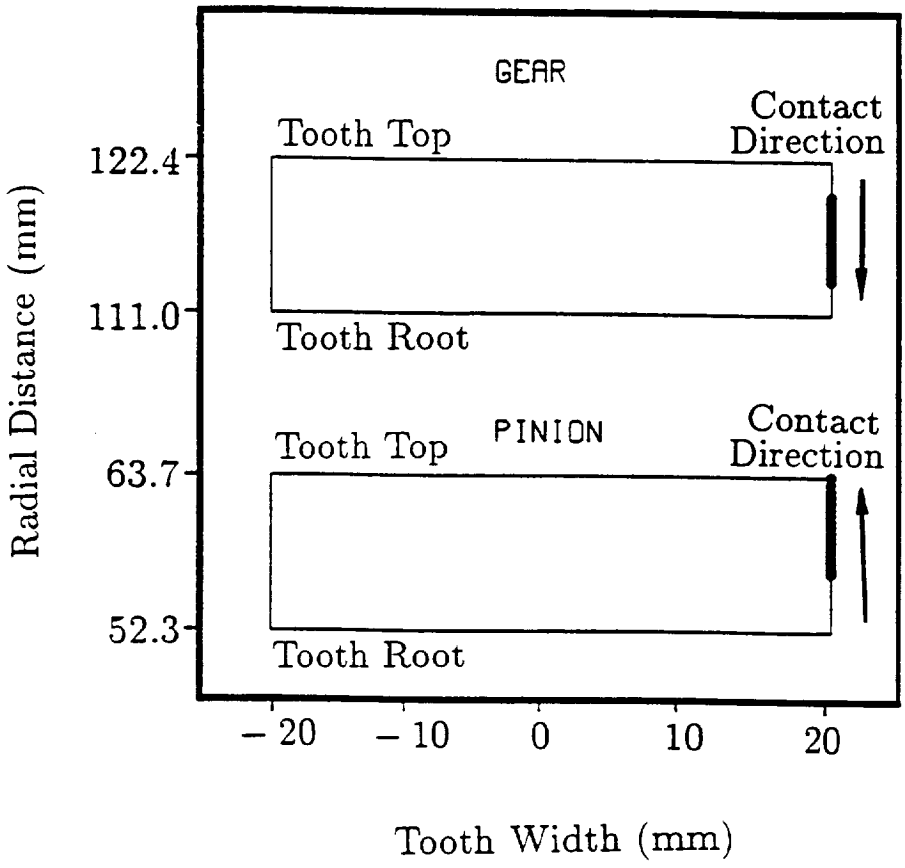

Fig. 1 Edge contact of helical gears: error of crossing angle is $\triangle\gamma = 5.0arc - min$

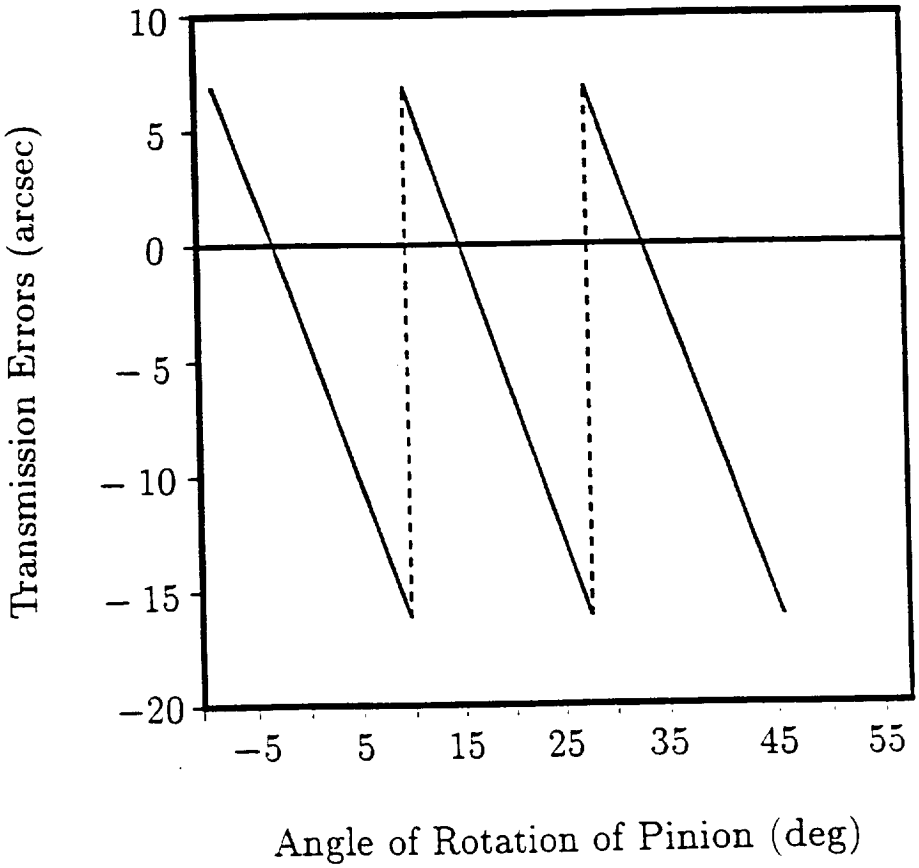

Fig. 2 Transmission errors of helical gears: error of crossing angle is $\Delta\gamma = 5.0arc - min$

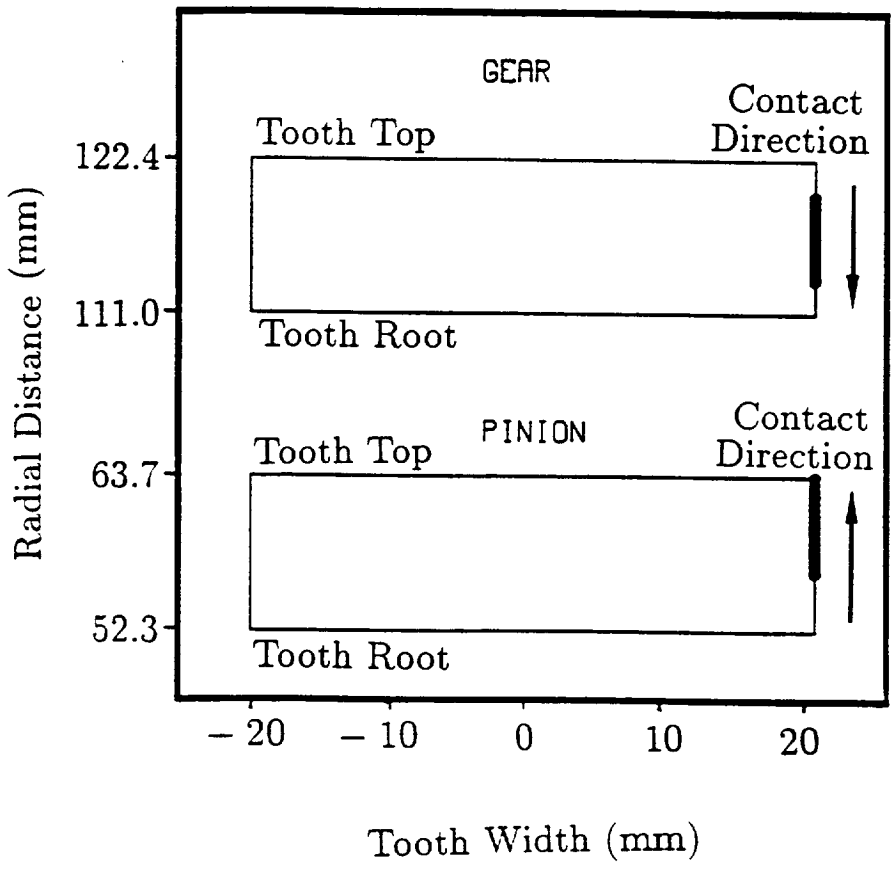

Fig. 3 Edge contact of helical gears: error of pinion lead angle on pitch cylinder is $\triangle\lambda_{pl} = 5.0arc - min$

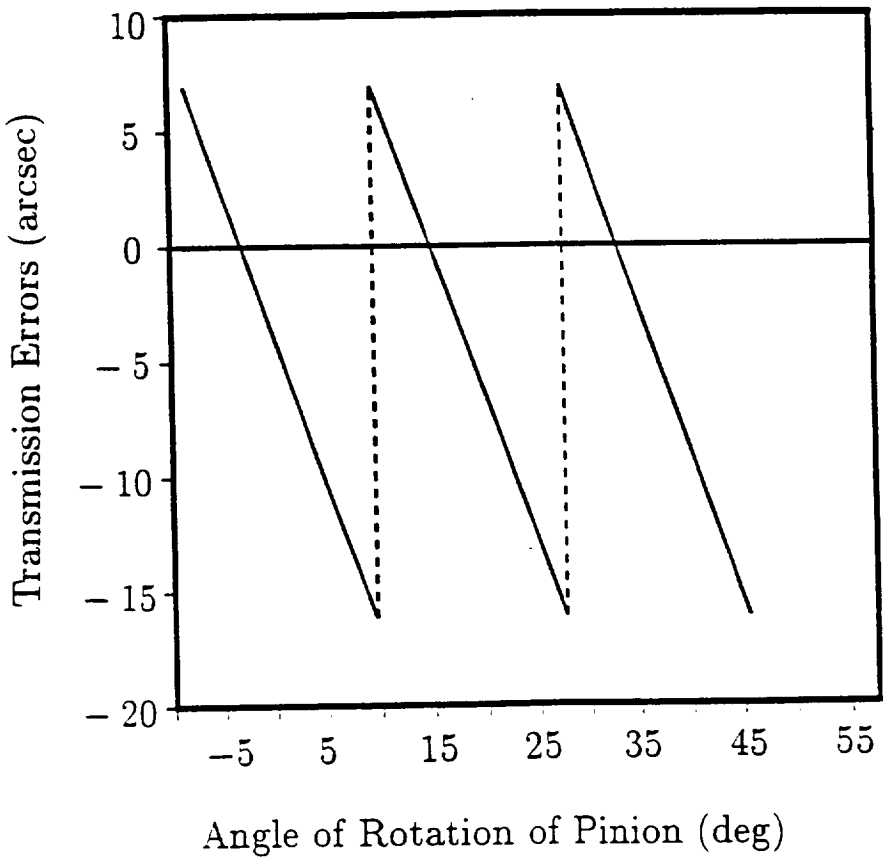

Fig. 4 Transmission error of helical gears: error of pinion lead angle on pitch cylinder is $\Delta\lambda_{p1} = 5.0arc - min$

Δ E = 0.2 mm

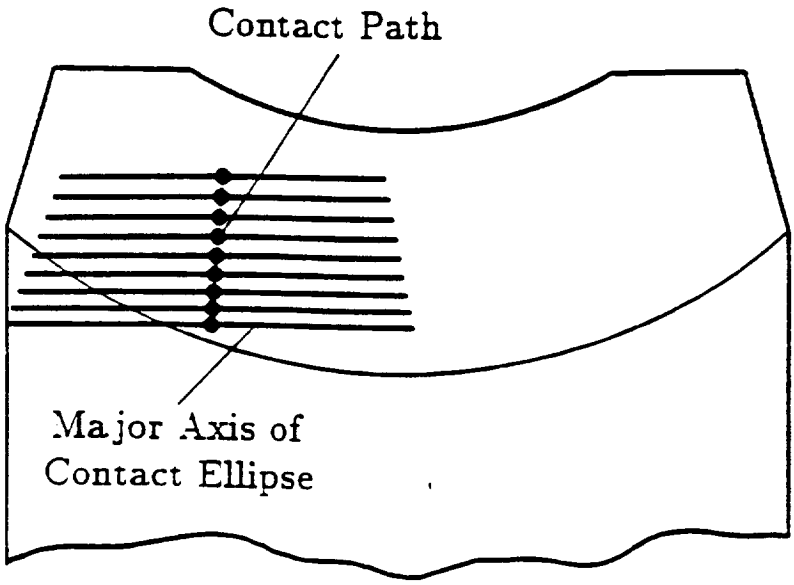

Fig. 5 Shift of bearing contact due to change of center distance $\triangle E = 0.2mm$

Δ E = 0.5 mm
$\Delta\gamma$ = 5'

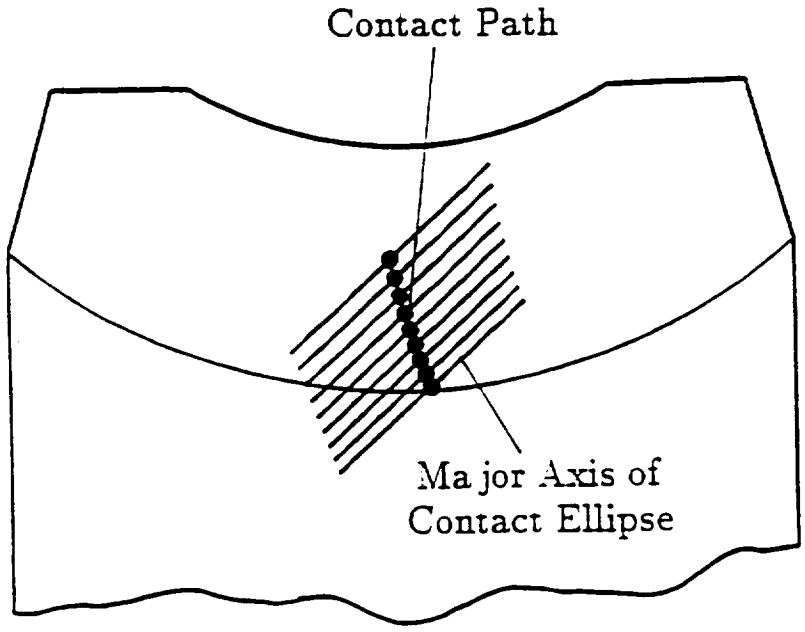

Fig. 6 Shift of bearing contact due to change of center distance ΔE and crossing angle $\Delta\gamma$

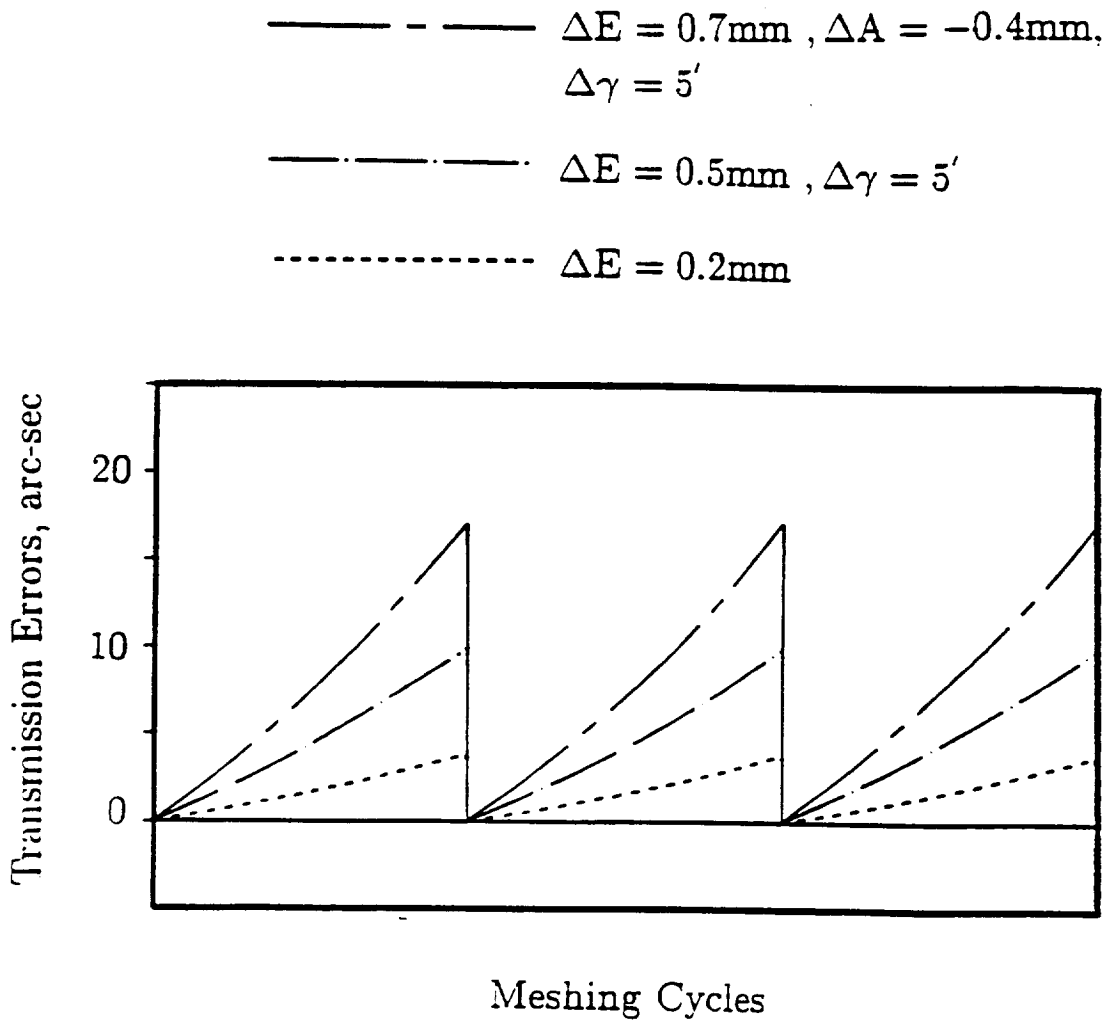

Fig. 7 Transmission errors of misaligned worm-gear drive

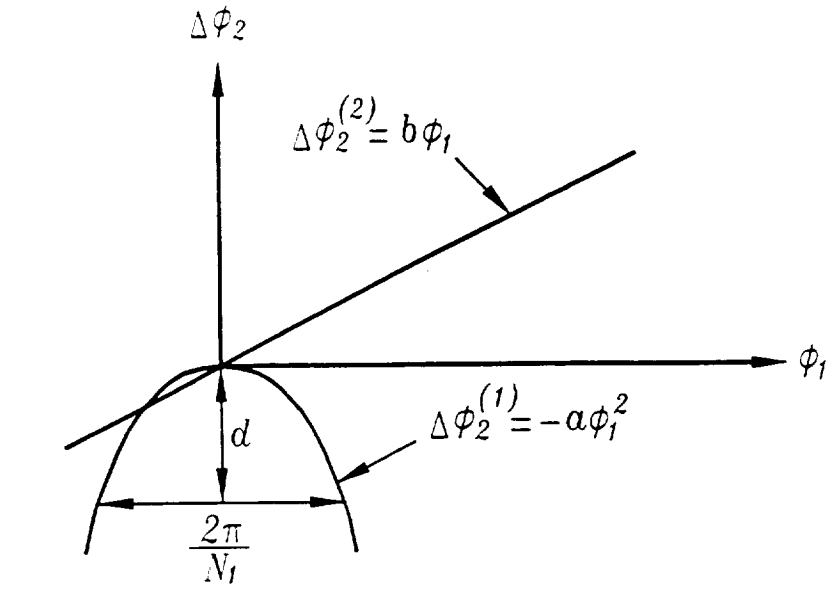

(a)

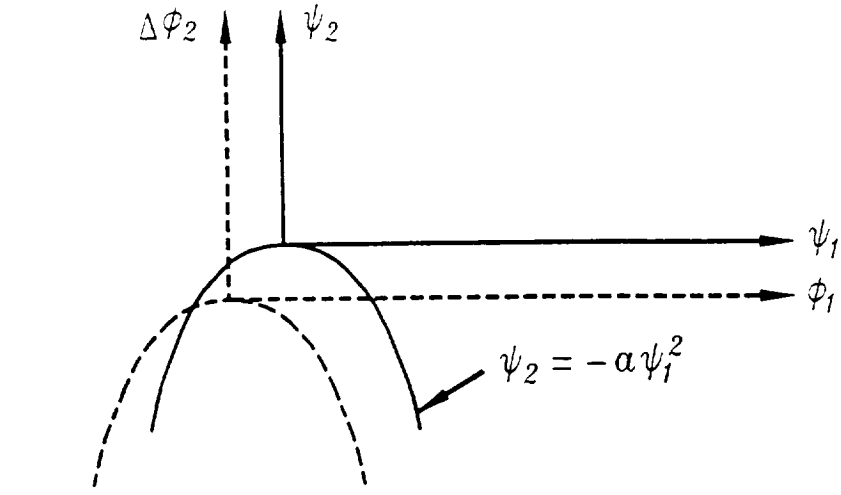

(b)

Fig. 8 Interaction of parabolic and linear functions

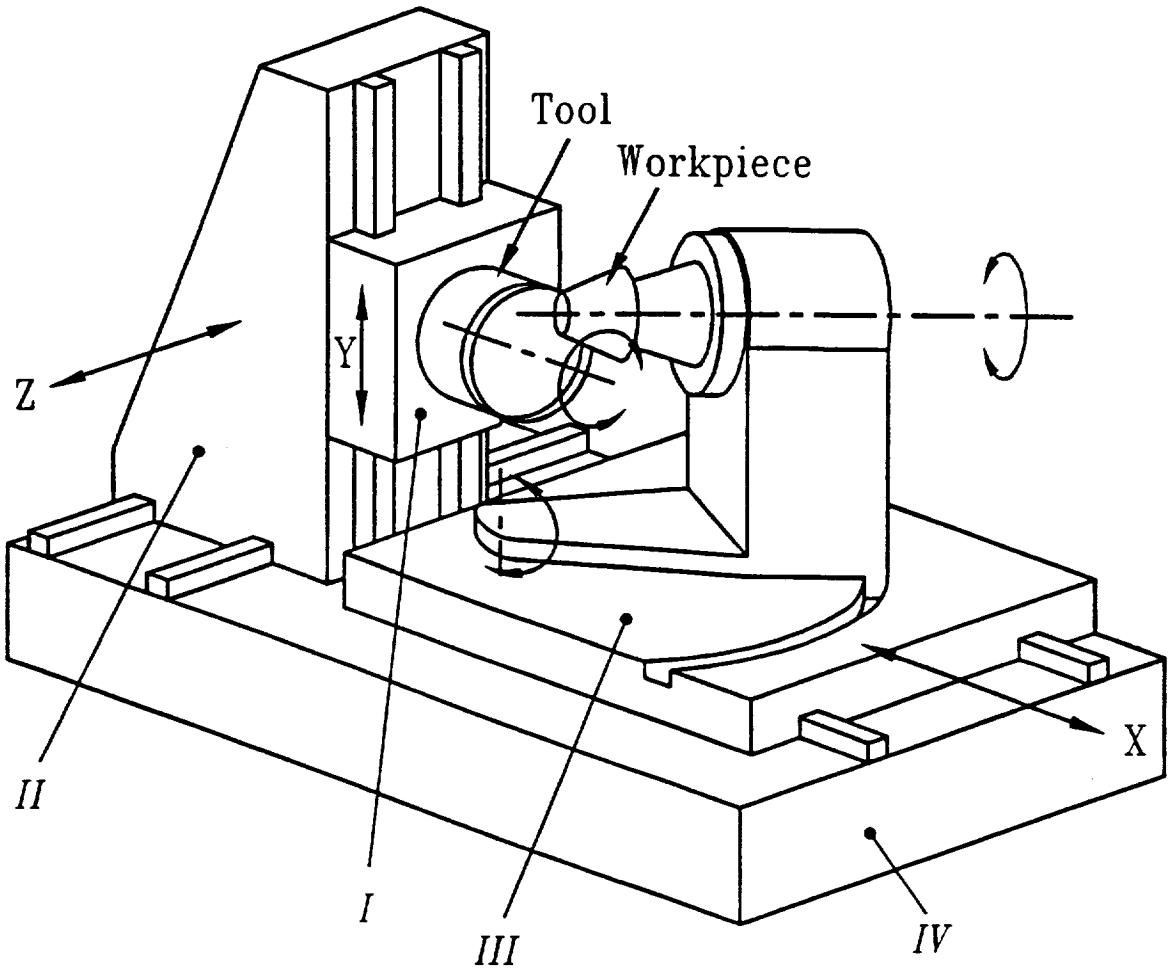

Fig. 9 Schematic of "Phoenix" machine

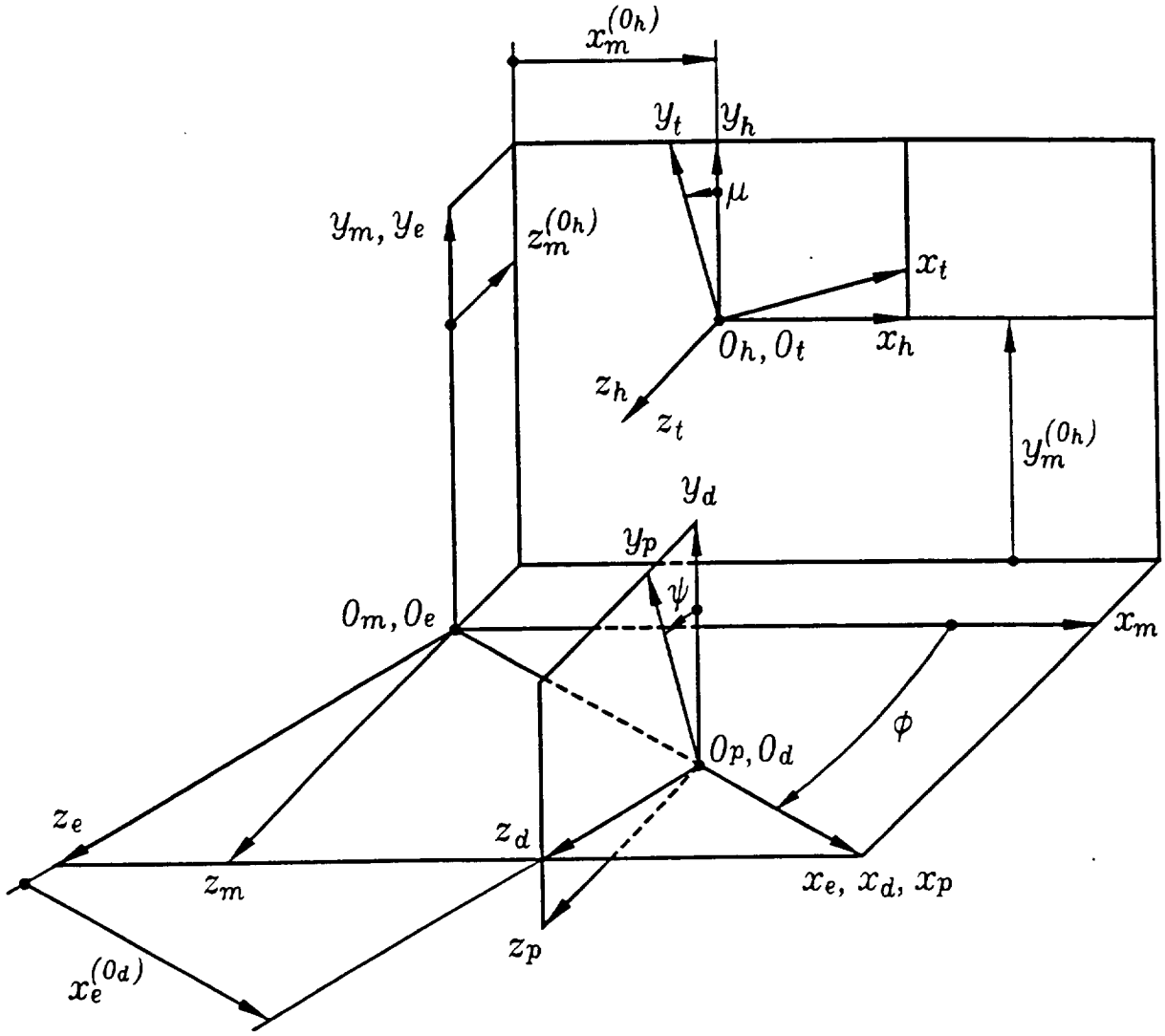

Fig. 10 Coordinate systems applied to "Phoenix" machine

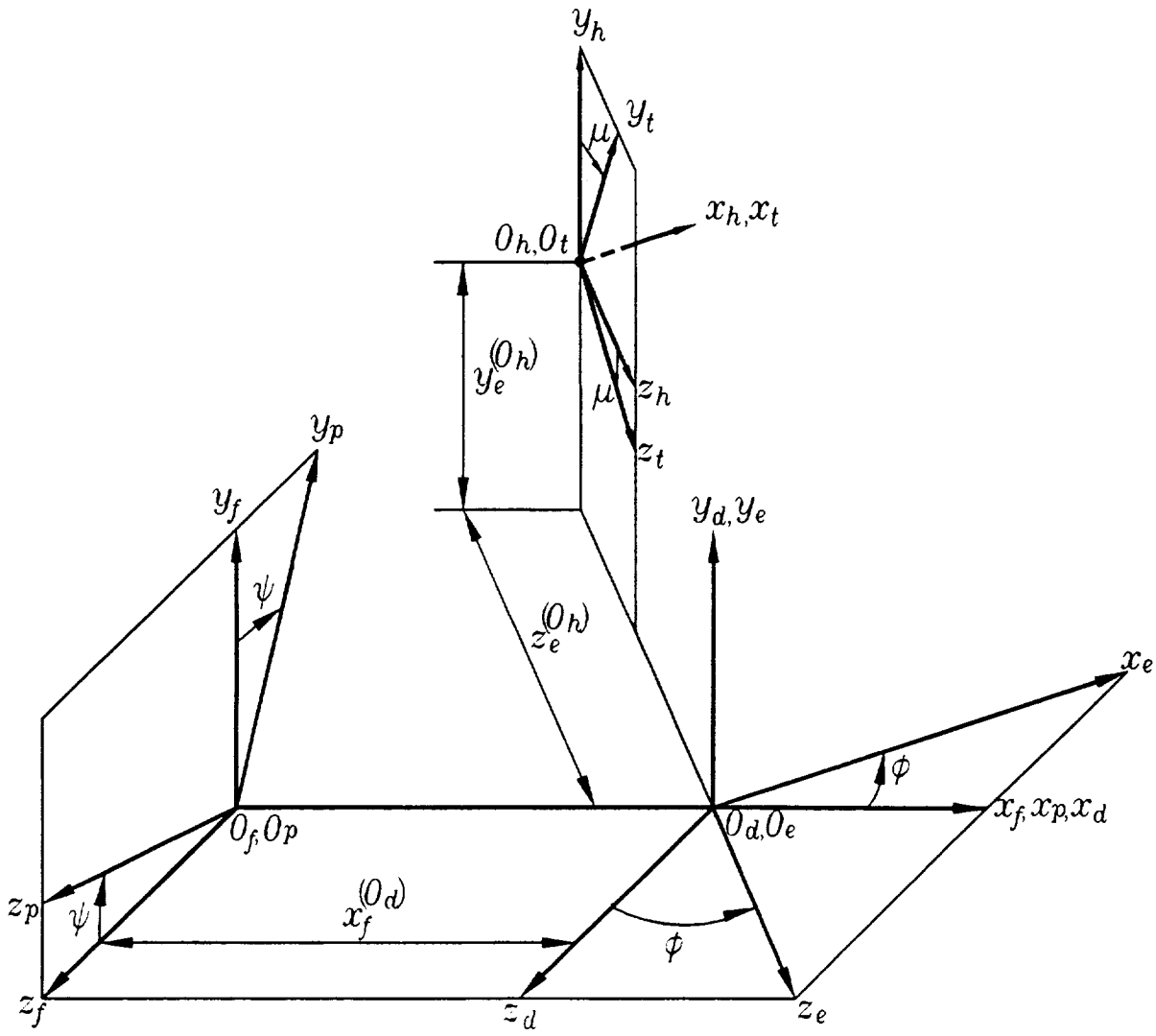

Fig. 11 "Star" CNC machine

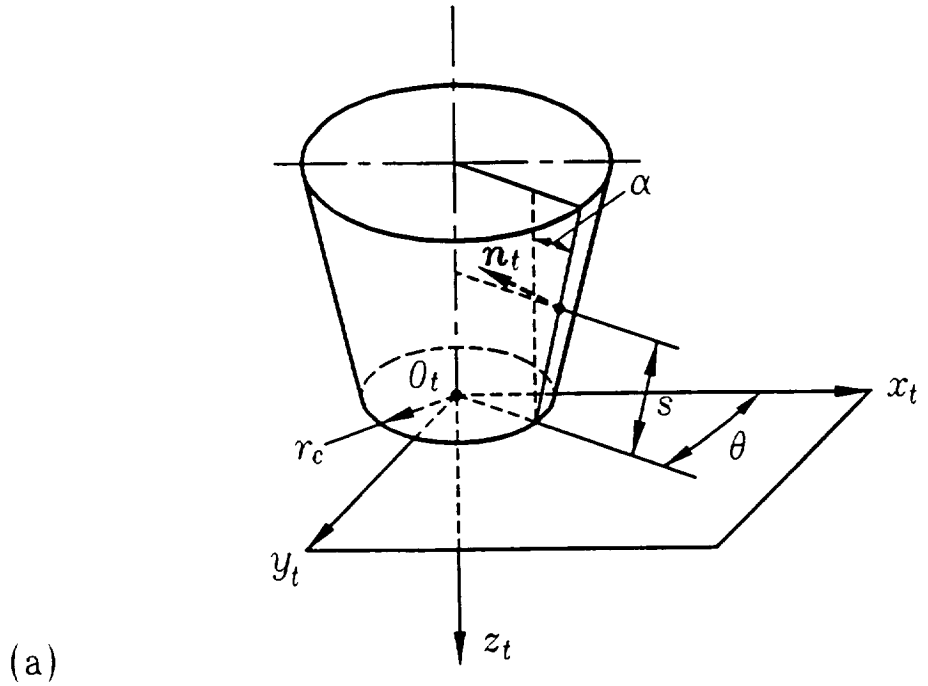

(a)

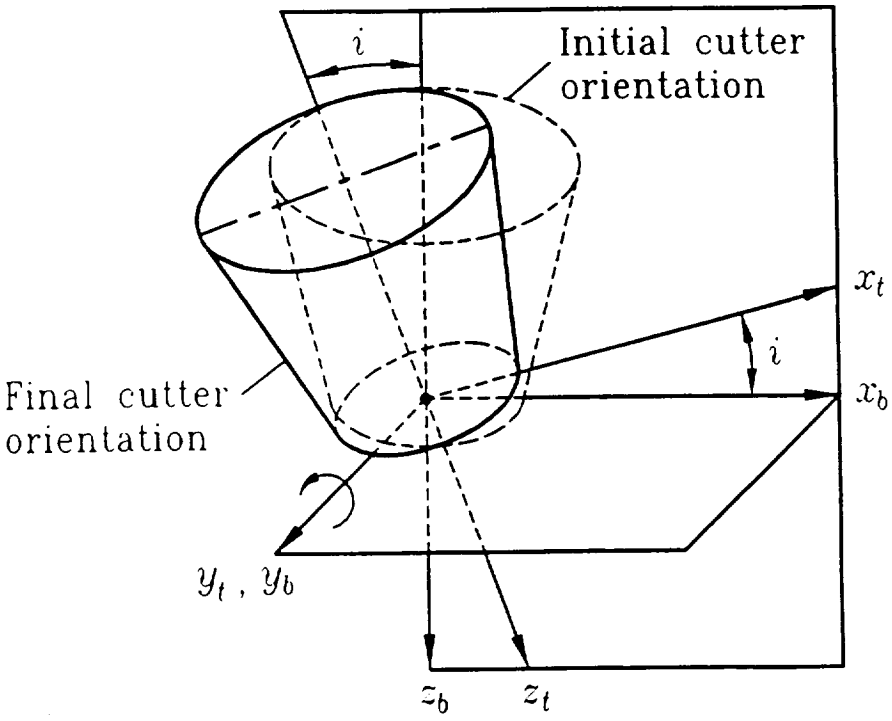

(b) i – tilt angle

Fig. 12 Pinion head-cutter

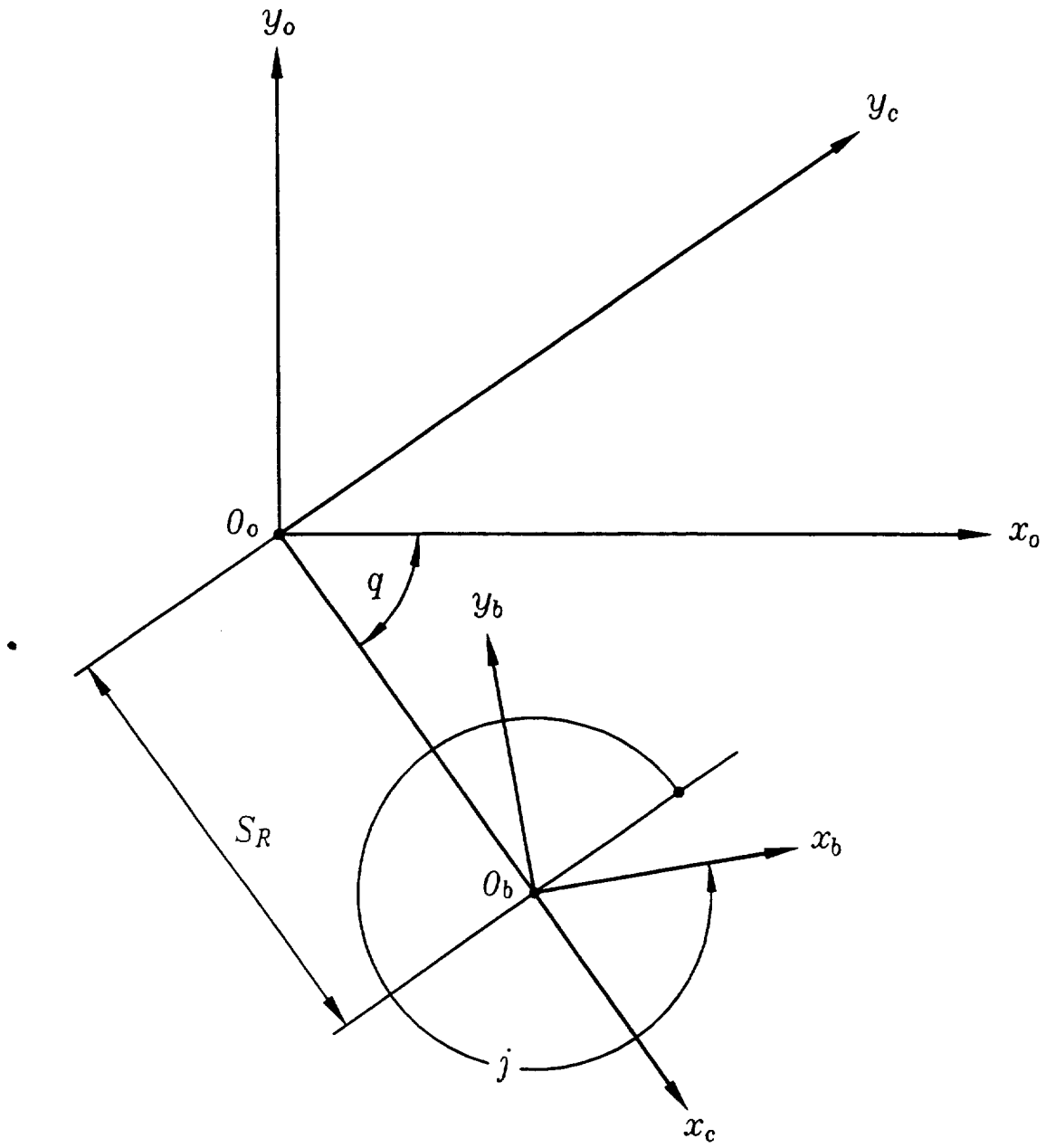

Fig. 13 Coordinate systems S_o, S_c and S_b.

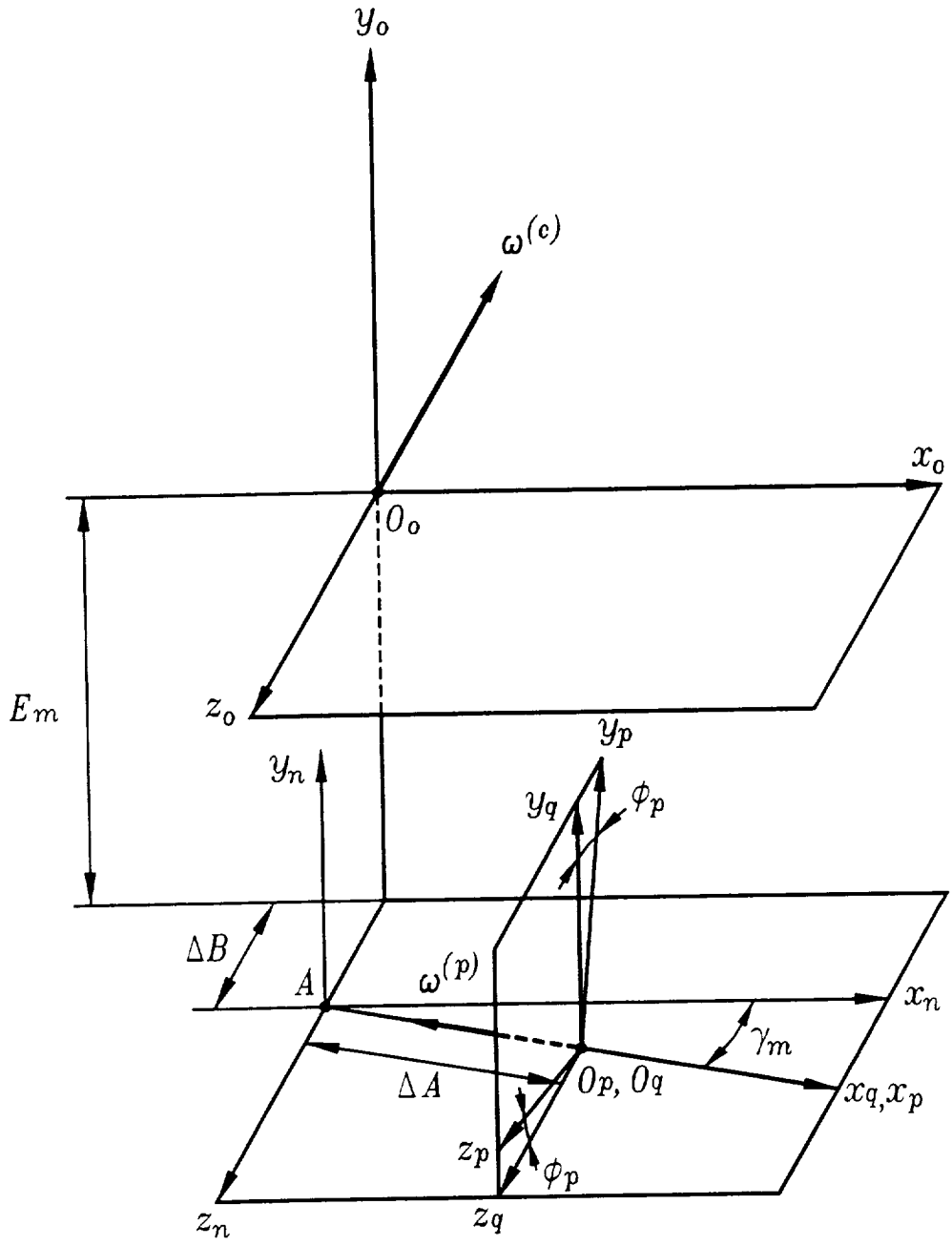

Fig. 14 Pinion generation

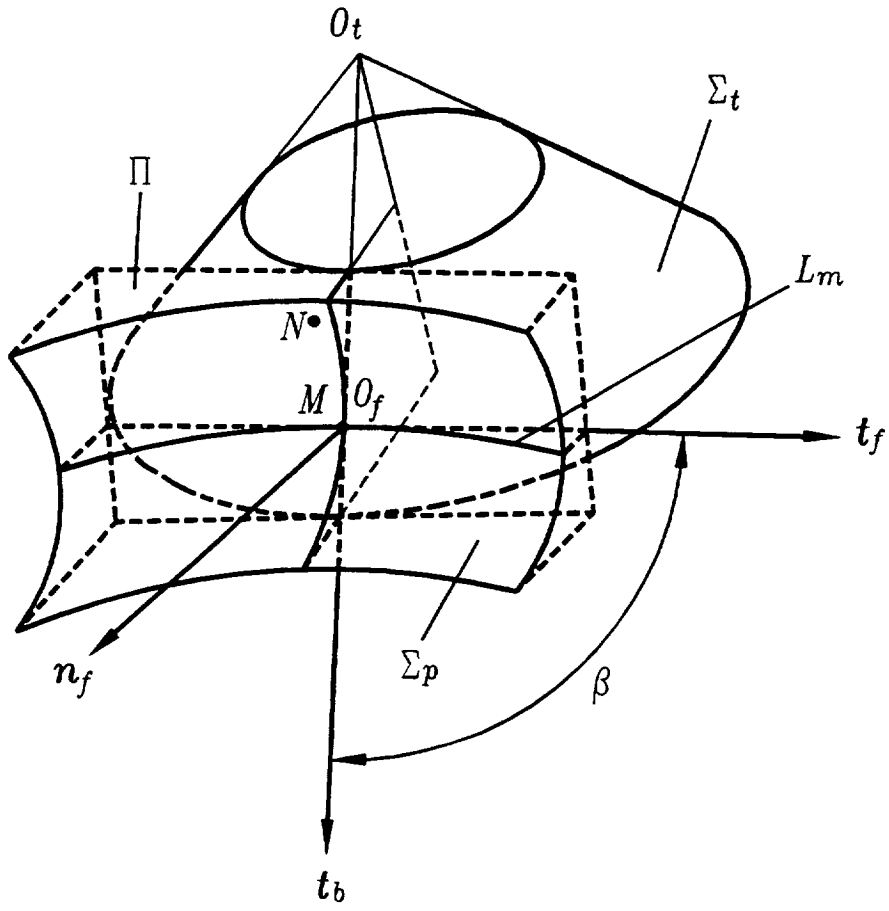

Fig. 15 Installment and orientation of tool surface Σ_t with respect to ideal surface Σ_p

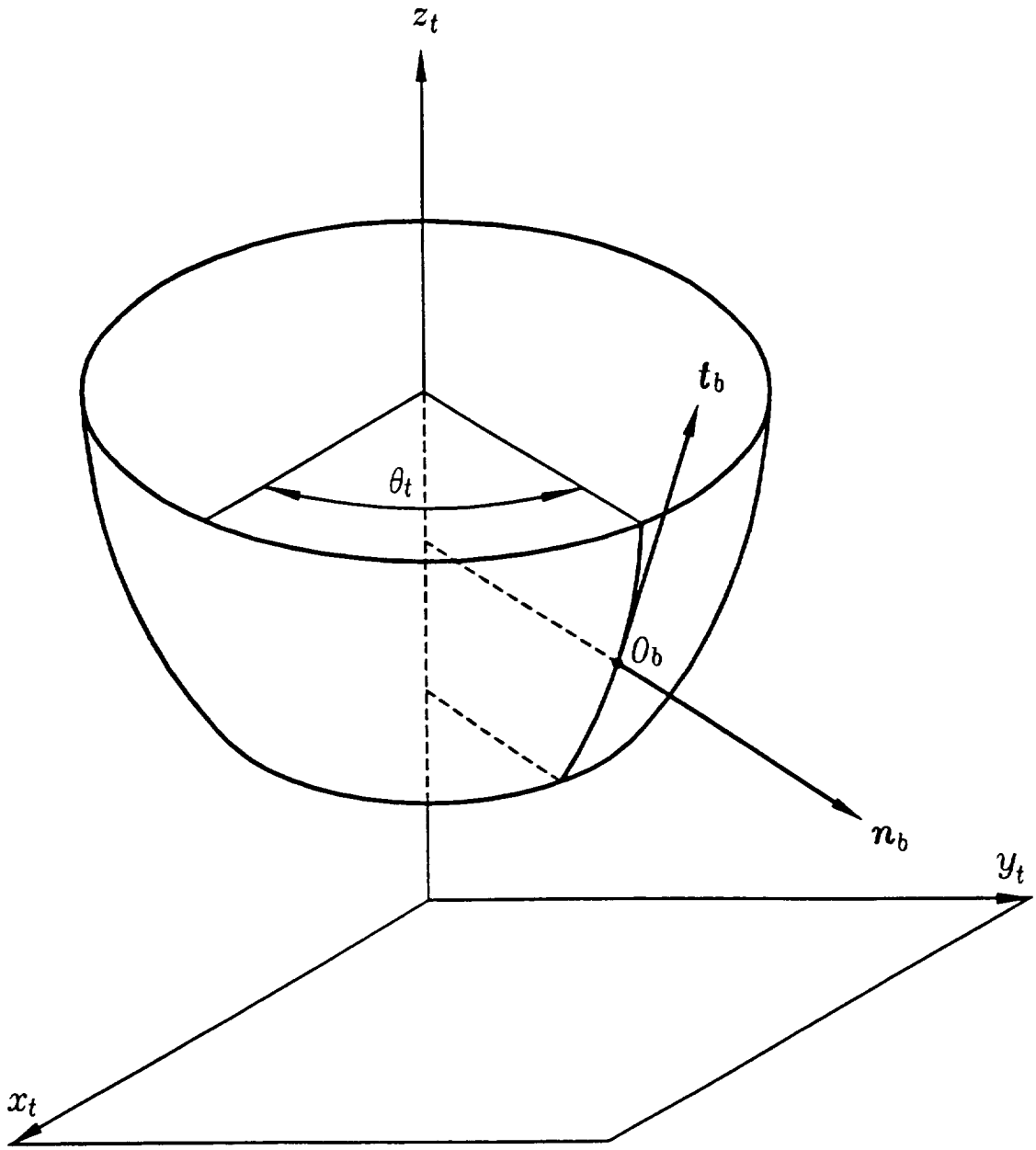

Fig. 16 Tool surface Σ_t

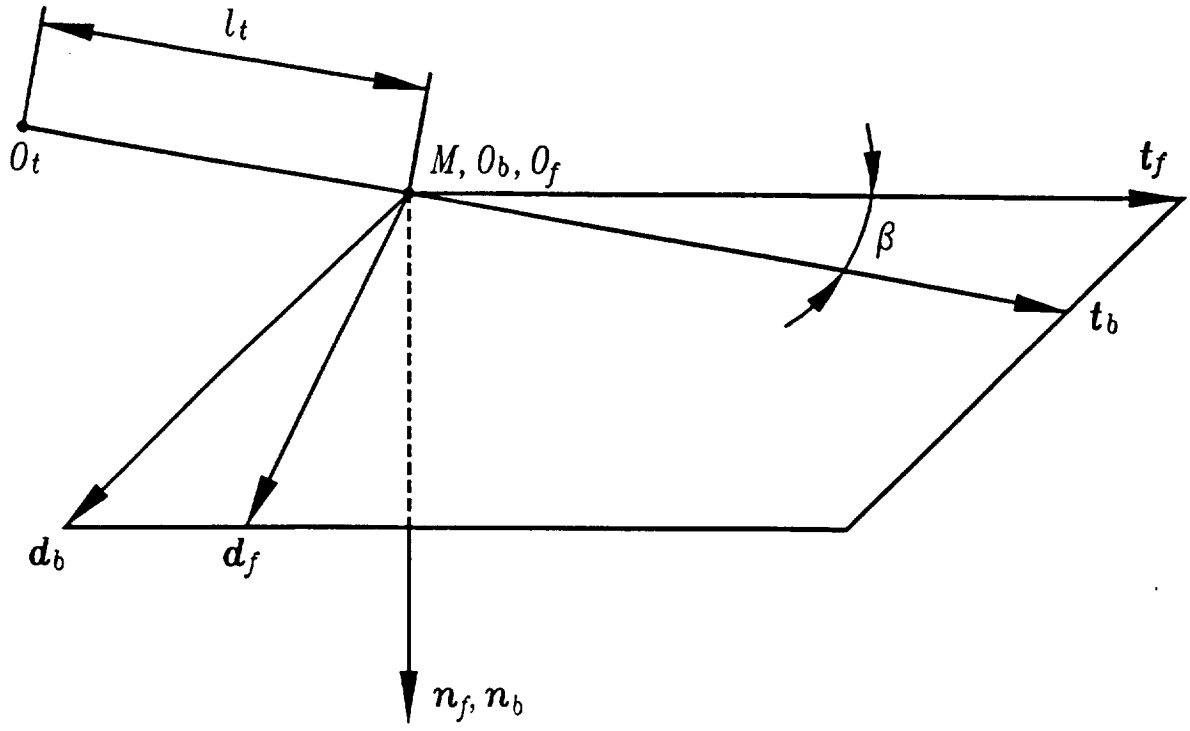

Fig. 17 Orientation of trihedron S_b with respect to S_f

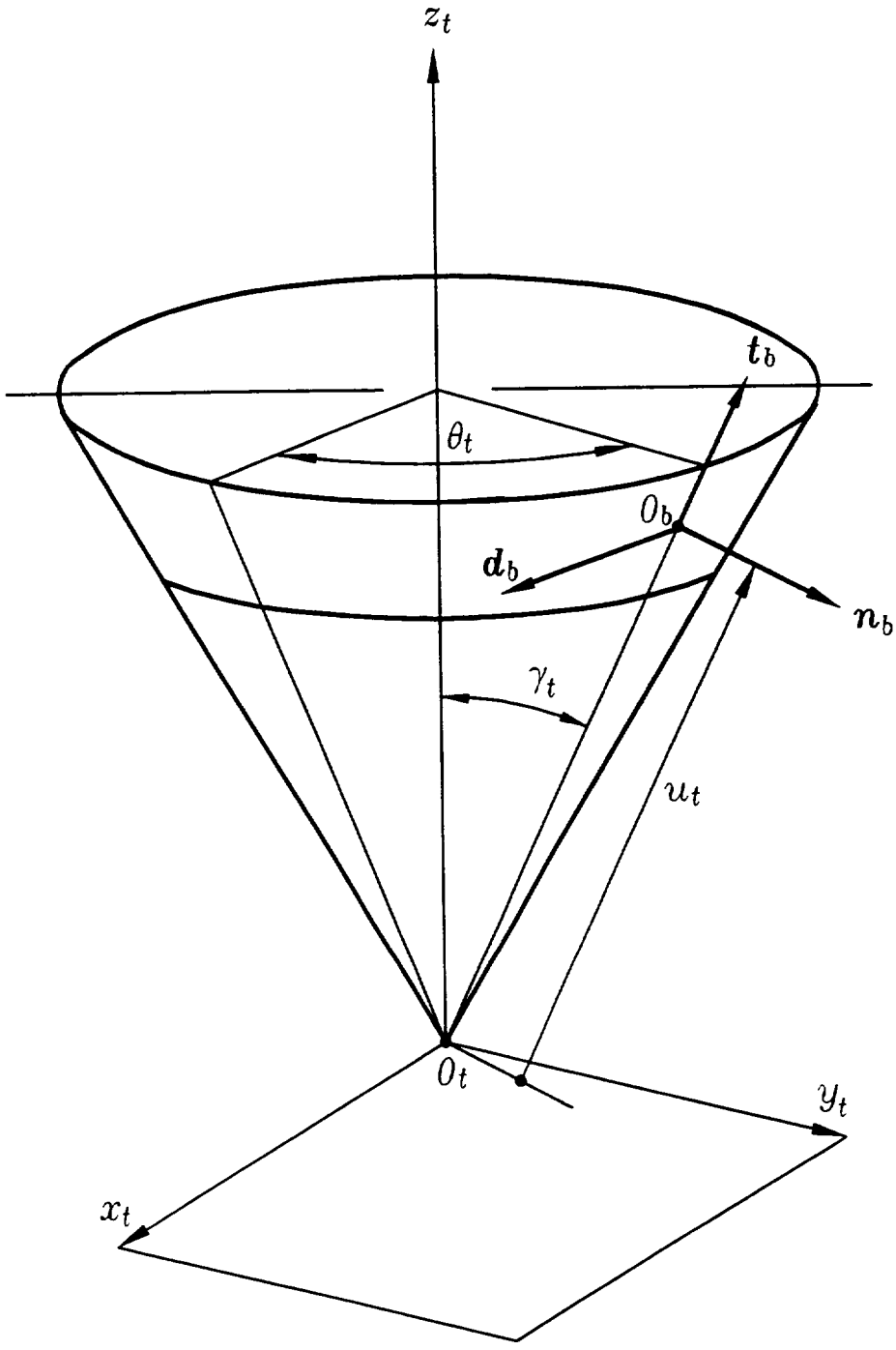

Fig. 18 Surface of grinding tool cone

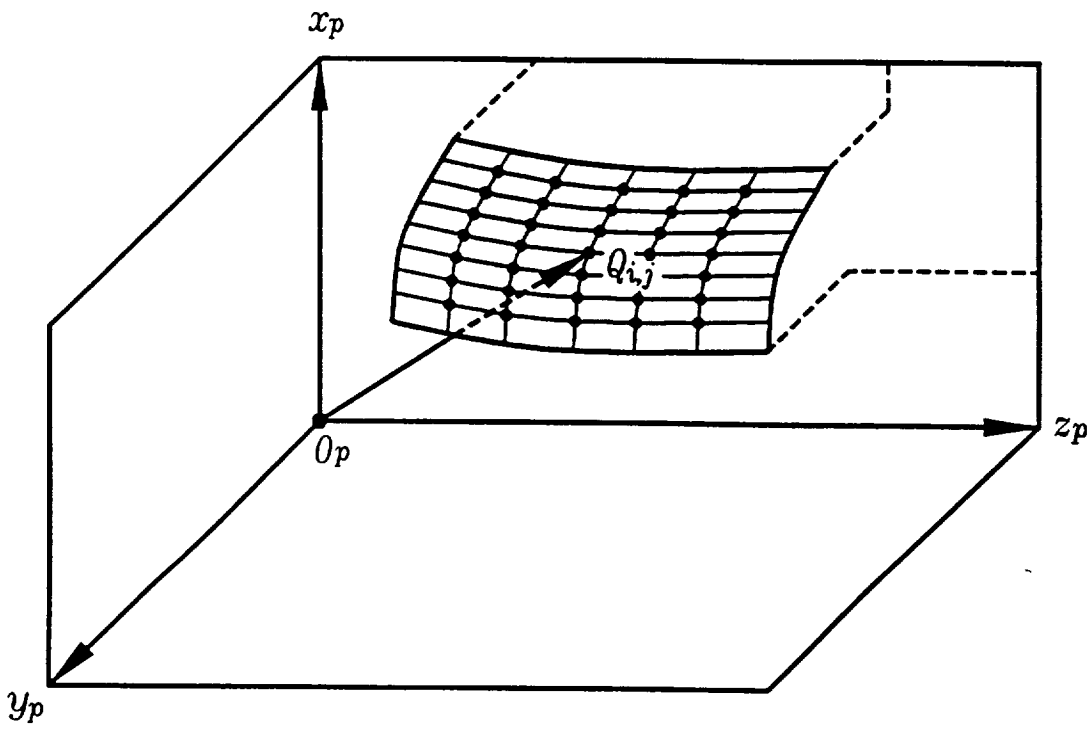

(a)

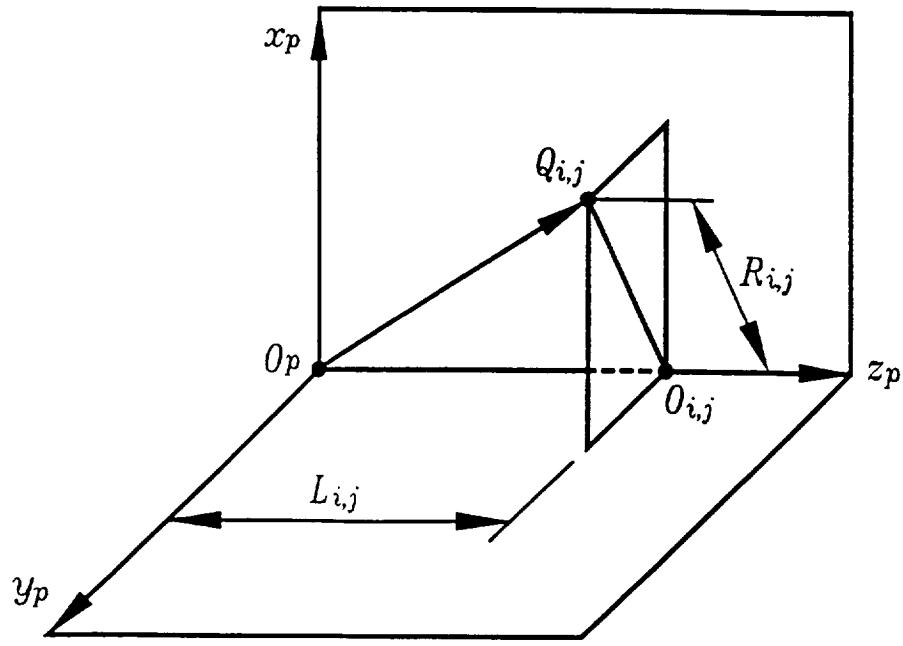

(b)

Fig. 19 Grid on surface Σ_p

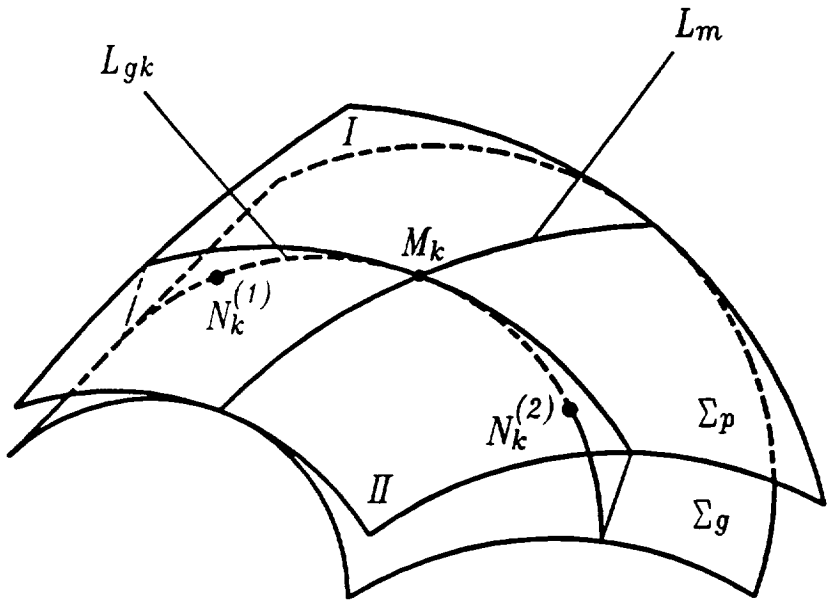

Fig. 20 Determination of maximum derivations along line L_{gk}

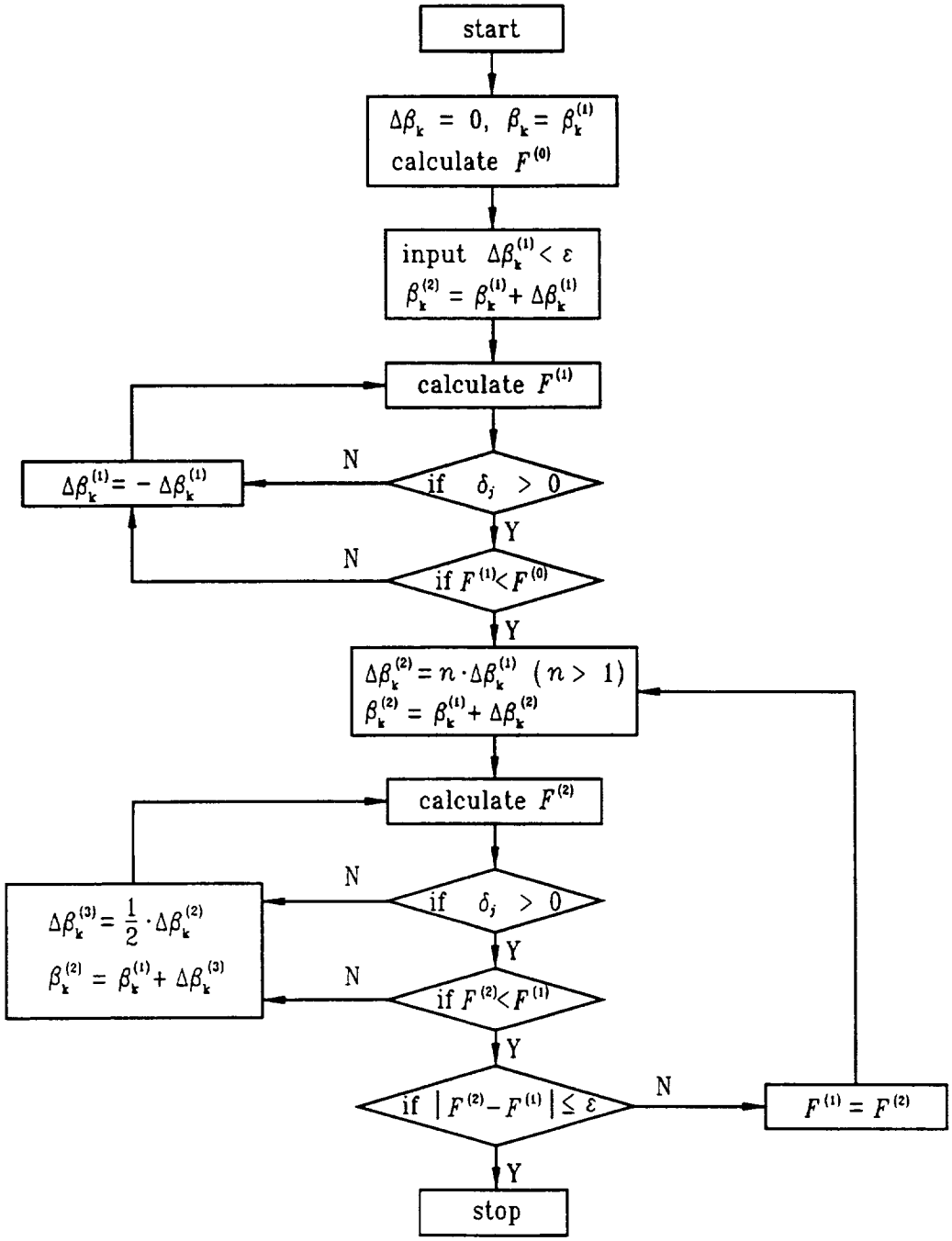

Fig. 21 Flow chart for optimization

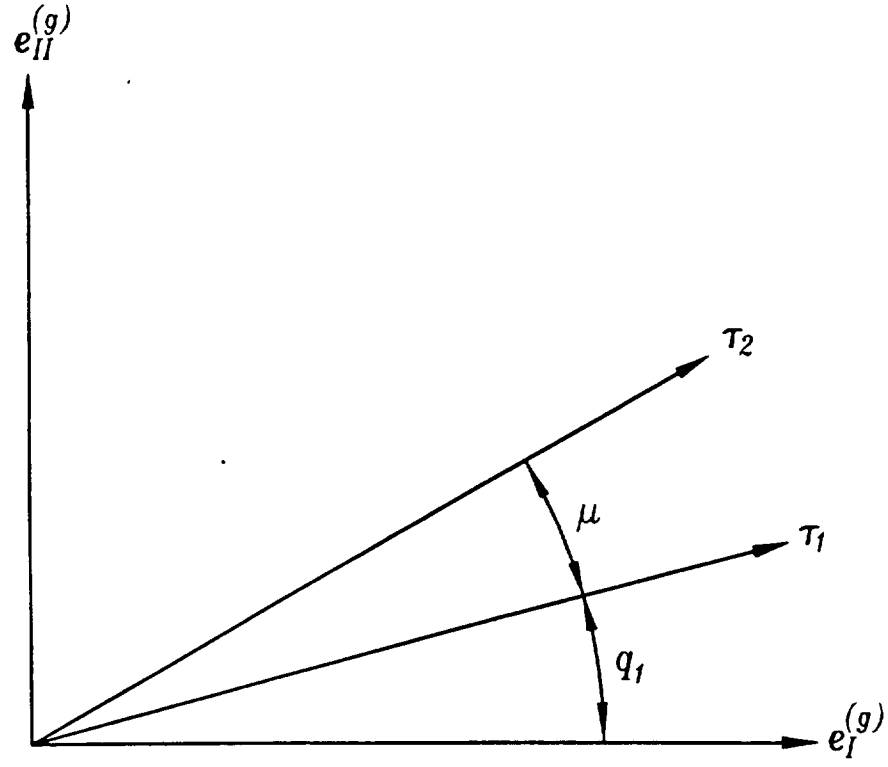

Fig. 22 To determination of principal directions of generated surface Σ_g

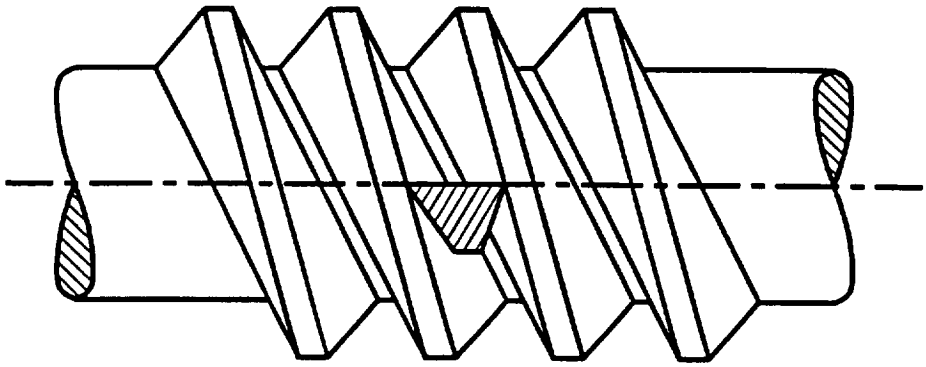

(a)

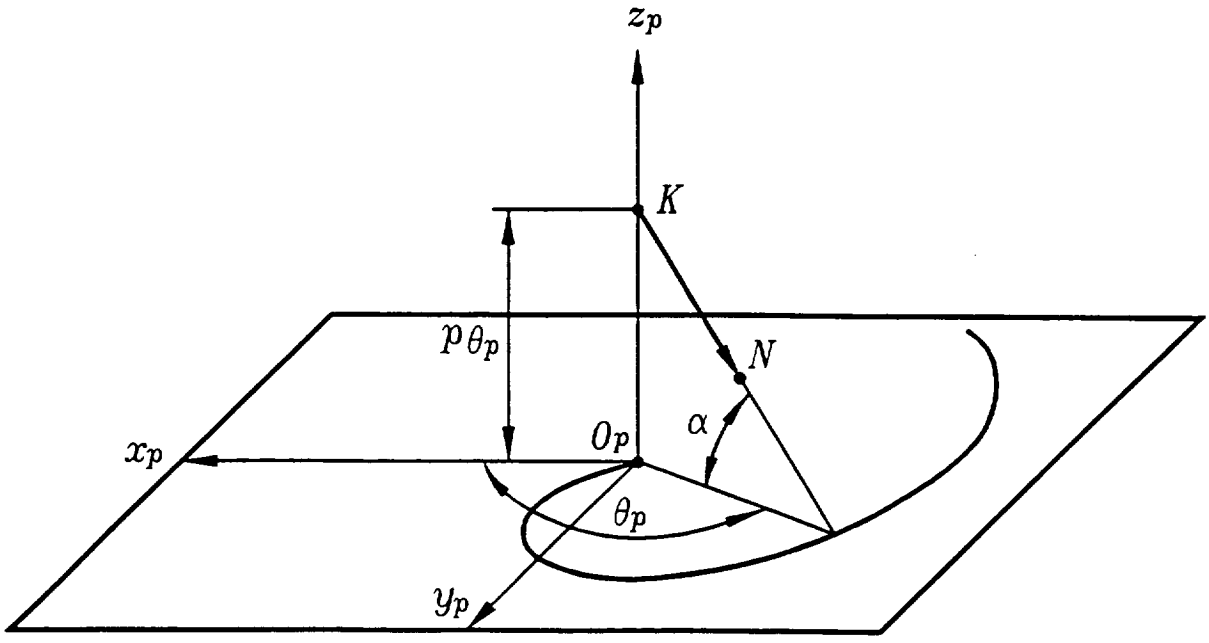

(b)

Fig. 23 Surface of Archimedes' worm

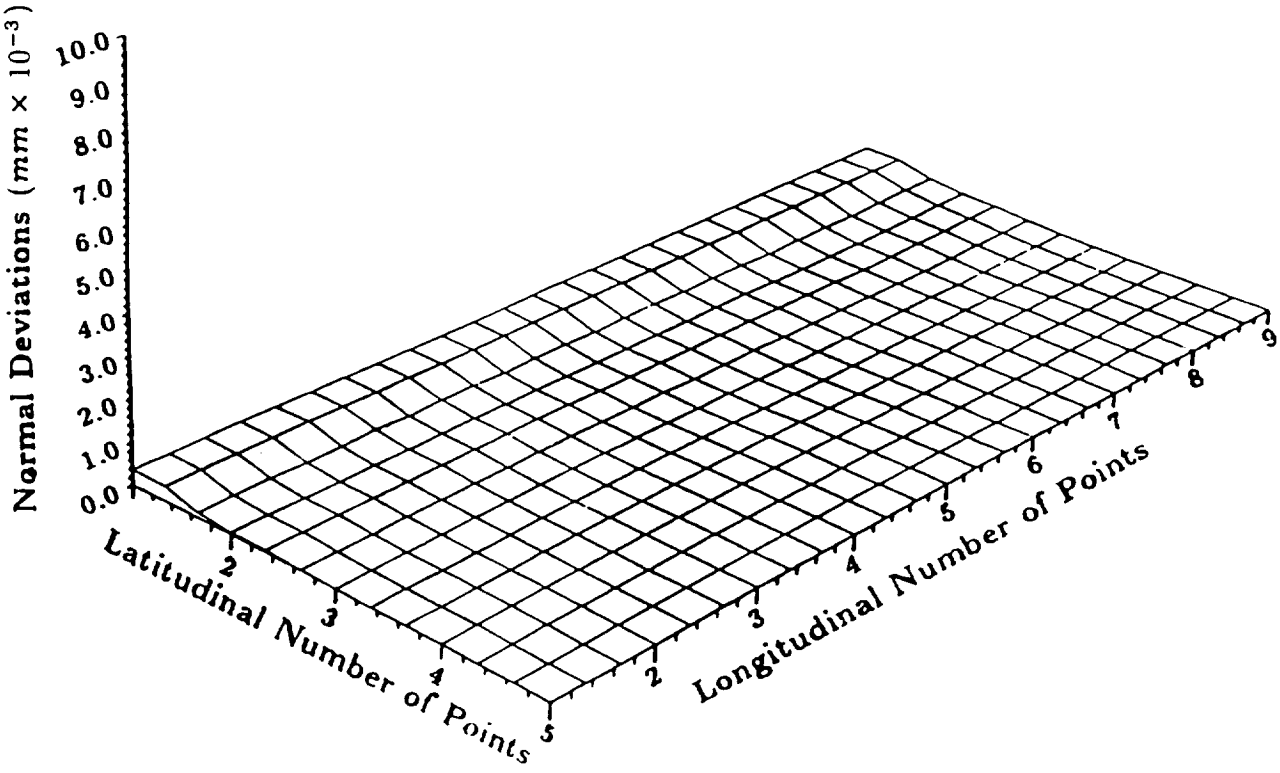

Fig. 24 Deviations of the ground surface Σ_g from ideal surface Σ_p of Archimedes' worm

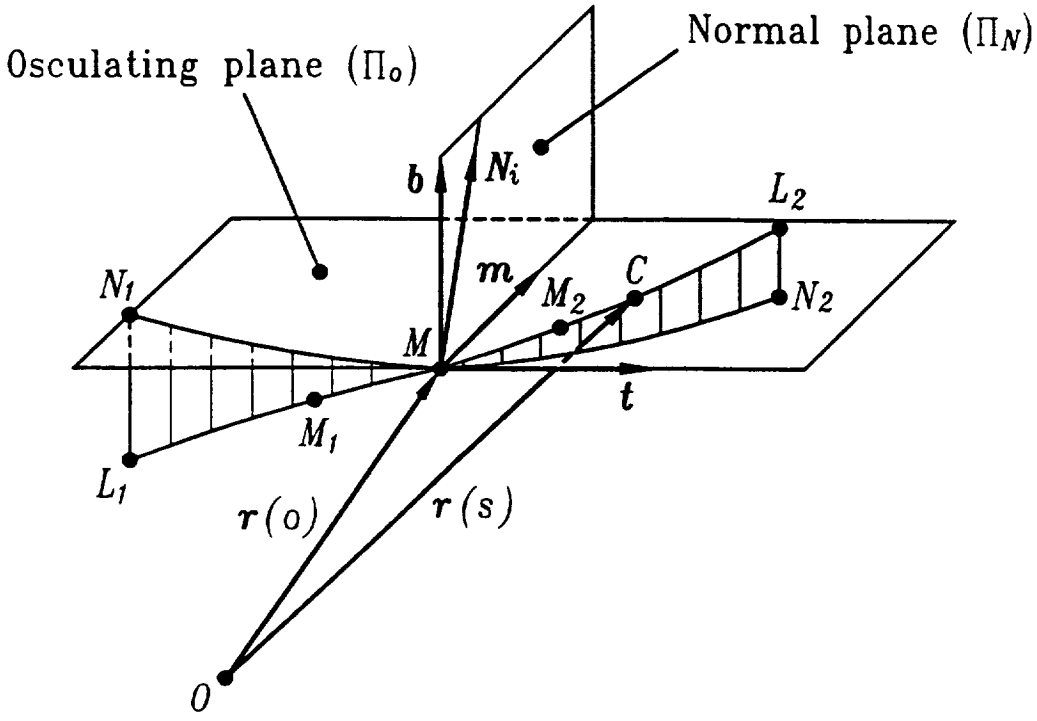

Fig. 25 Osculating and normal planes

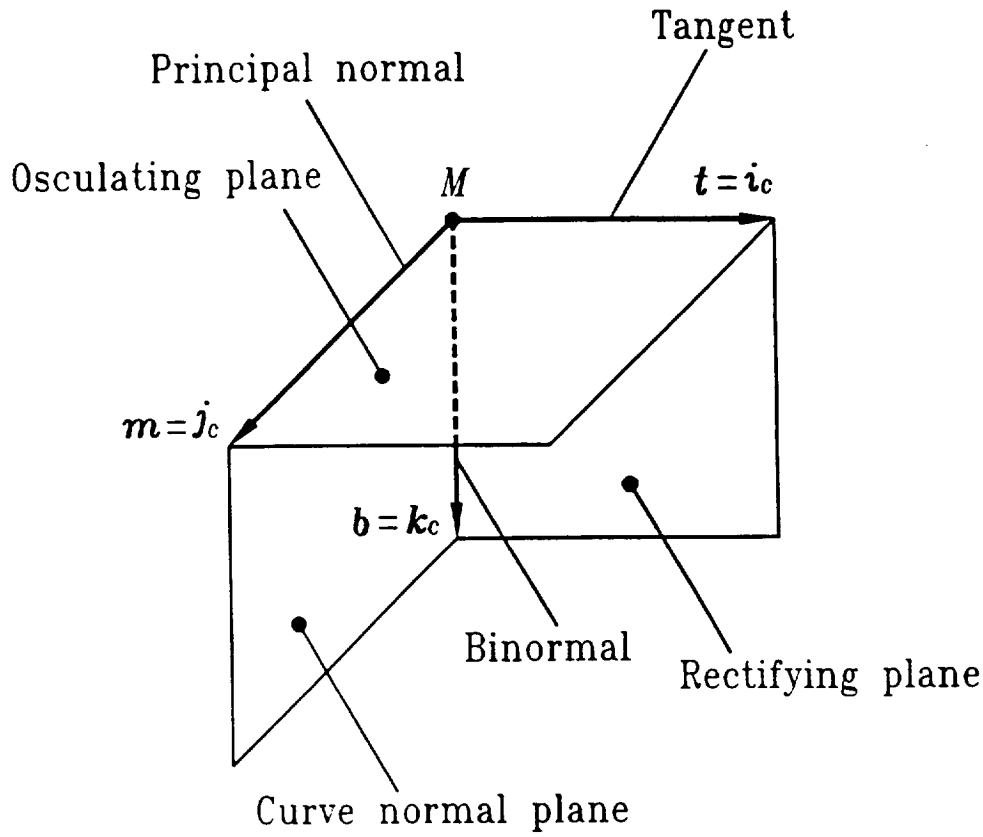

Fig. 26 Curve trihedron

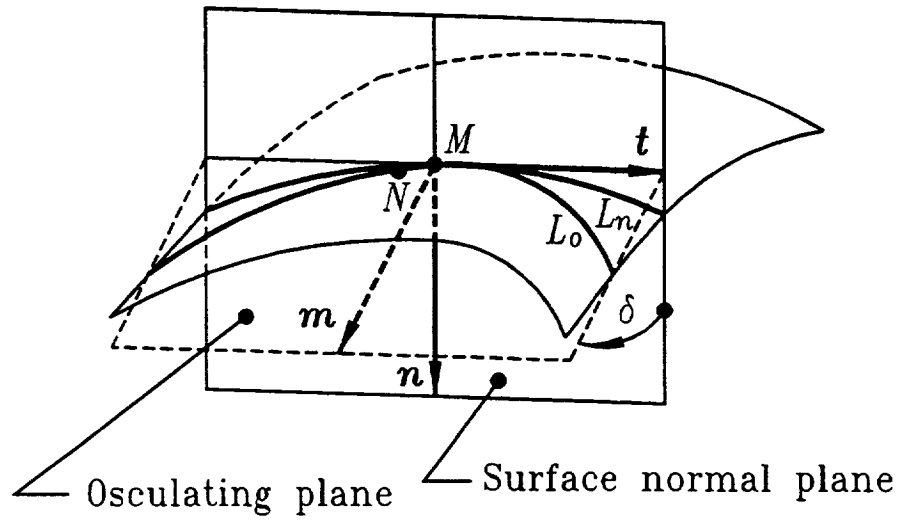

(a)

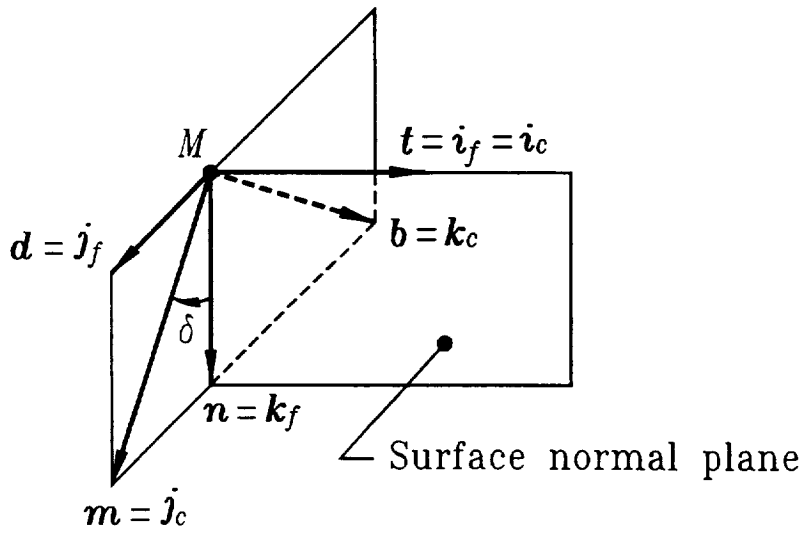

(b)

Fig. 27 Surface trihedron

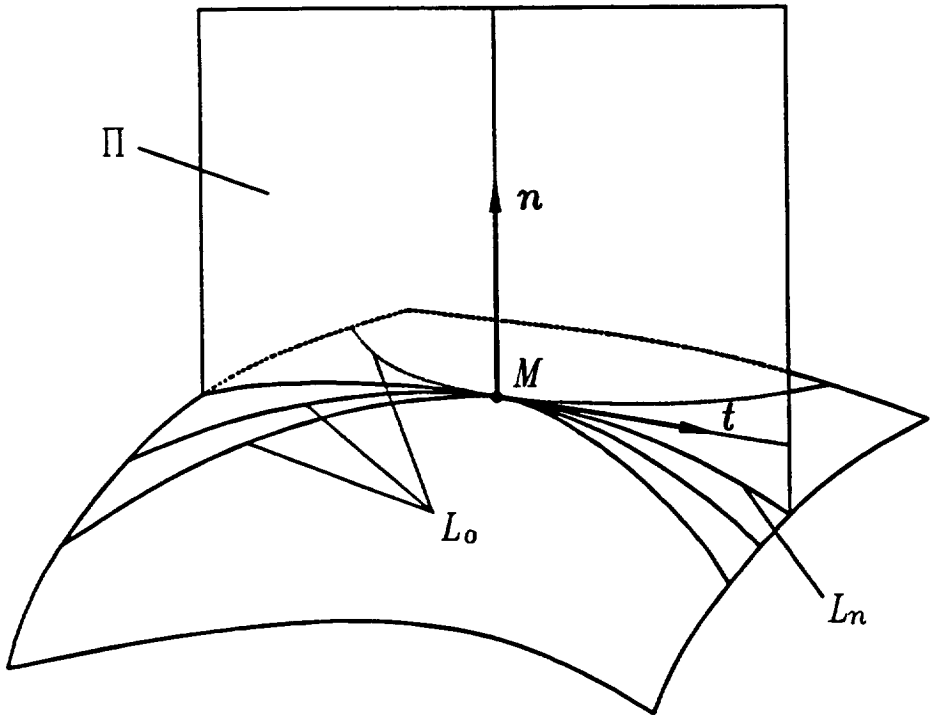

Fig. 28 Surface normal section and surface spatial curves

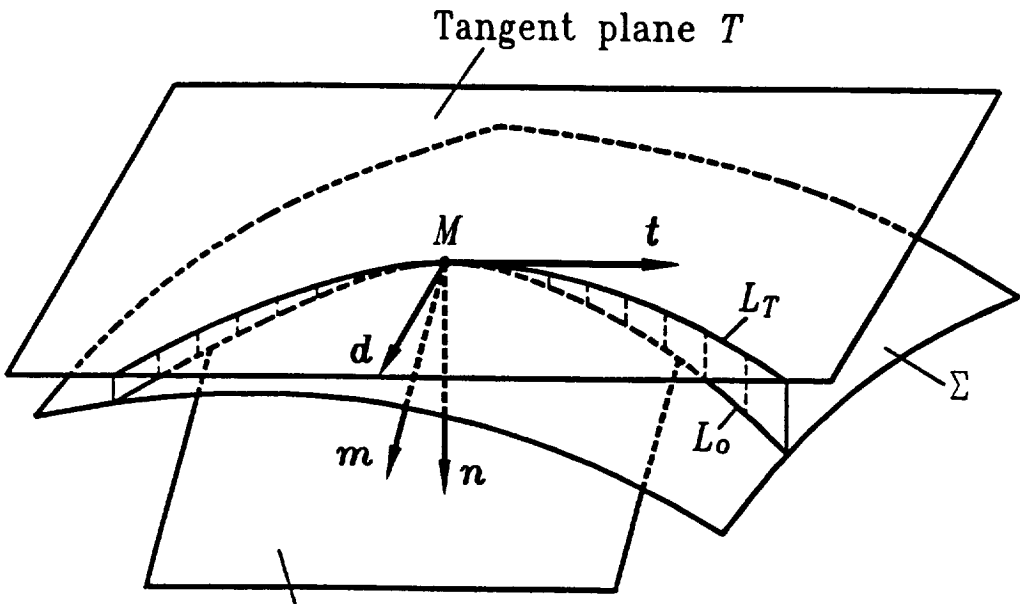

(a)

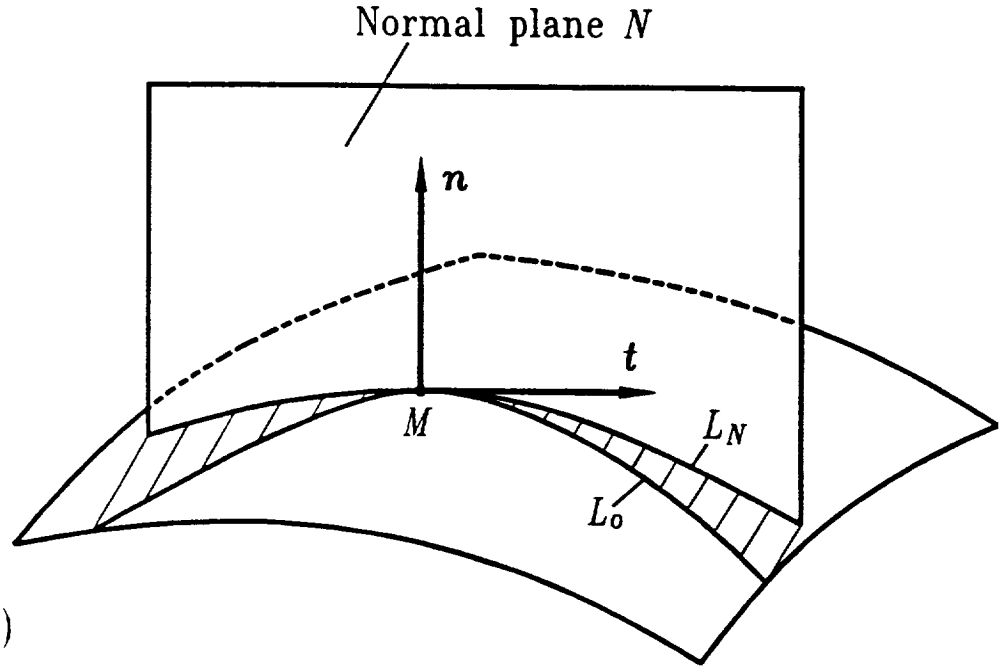

(b)

Fig. 29 Normal and geodesic curvatures

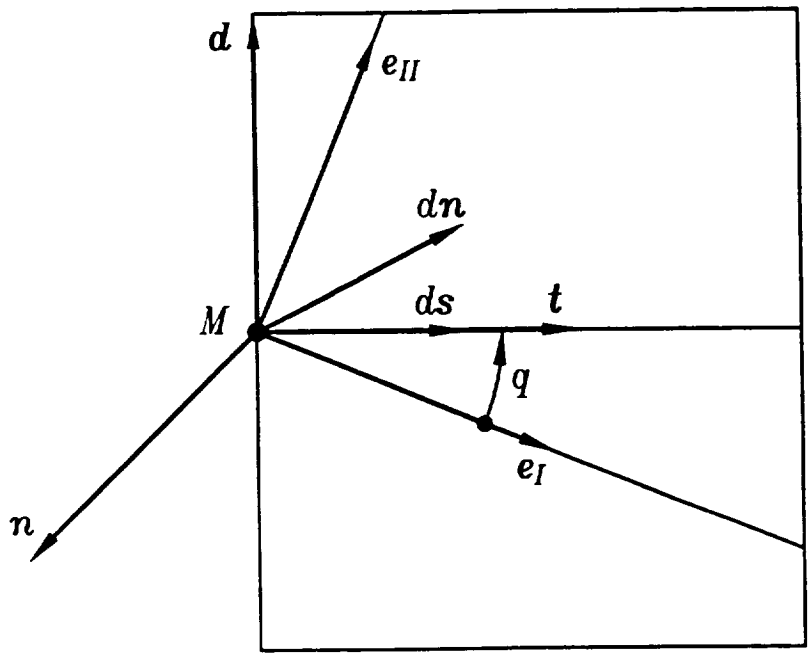

Fig. 30 Interpretation of the surface torsion

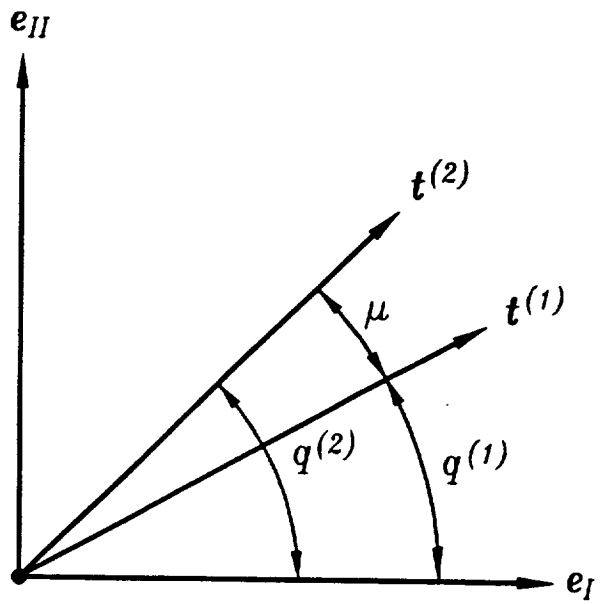

Fig. 31 Surface principal directions and directions of tangents to two surface curves

REPORT DOCUMENTATION PAGE

Form Approved
OMB No. 0704-0188

1. AGENCY USE ONLY (*Leave blank*)	2. REPORT DATE	3. REPORT TYPE AND DATES COVERED
	April 1994	Final Contractor Report

4. TITLE AND SUBTITLE

Generation of Gear Tooth Surfaces by Application of CNC Machines

5. FUNDING NUMBERS

WU-505-62-36
1L162211A47A

6. AUTHOR(S)

F.L. Litvin and N.X. Chen

7. PERFORMING ORGANIZATION NAME(S) AND ADDRESS(ES)

University of Illinois at Chicago
Chicago, Illinois 60680

8. PERFORMING ORGANIZATION REPORT NUMBER

E-8712

9. SPONSORING/MONITORING AGENCY NAME(S) AND ADDRESS(ES)

Vehicle Propulsion Directorate
U.S. Army Research Laboratory
Cleveland, Ohio 44135-3191
and
NASA Lewis Research Center
Cleveland, Ohio 44135-3191

10. SPONSORING/MONITORING AGENCY REPORT NUMBER

NASA CR-195306
ARL-CR-145

11. SUPPLEMENTARY NOTES

Project Manager, Robert F. Handschuh, Propulsion System Division, organization code 2730, (216) 433-3969.

12a. DISTRIBUTION/AVAILABILITY STATEMENT

Unclassified - Unlimited
Subject Category 37

12b. DISTRIBUTION CODE

13. ABSTRACT (*Maximum 200 words*)

This study will demonstrate the importance of application of CNC machines in generation of gear tooth surfaces with new topology. This topology decreases gear vibration and will extend the gear capacity and service life. A preliminary investigation by a tooth contact analysis(TCA) program has shown that gear tooth surfaces in line contact (for instance, involute helical gears with parallel axes, worm-gear drives with cylindrical worms etc.) are very sensitive to angular errors of misalignment that cause edge contact and an unfavorable shape of transmission errors and vibration. The new topology of gear tooth surfaces is based on the localization of bearing contact, and the synthesis of a predesigned parabolic function of transmission errors that is able to absorb a piecewise linear function of transmission errors caused by gear misalignment. The report will describe the following topics: (1) Description of kinematics of CNC machines with 6 degrees-of-freedom that can be applied for generation of gear tooth surfaces with new topology. (2) A new method for grinding of gear tooth surfaces by a cone surface or surface of revolution based on application of CNC machines. This method provides an optimal approximation of the ground surface to the given one. This method is especially beneficial when undeveloped ruled surfaces are to be ground. (3) Execution of motions of the CNC machine. The solution to this problem can be applied as well for the transfer of machine-tool settings from a conventional generator to the CNC machine. The developed theory required the derivation of a modified equation of meshing based on application of the concept of space curves, space curves represented on surfaces, geodesic curvature, surface torsion, etc. Condensed information on these topics of differential geometry is provided as well.

14. SUBJECT TERMS	15. NUMBER OF PAGES
Gears; Gear teeth	84
	16. PRICE CODE: A05

17. SECURITY CLASSIFICATION OF REPORT	18. SECURITY CLASSIFICATION OF THIS PAGE	19. SECURITY CLASSIFICATION OF ABSTRACT	20. LIMITATION OF ABSTRACT
Unclassified	Unclassified		

National Aeronautics and
Space Administration

Lewis Research Center
21000 Brookpark Rd.
Cleveland, OH 44135-3191